

# A New Indium Phase with Three Stuffed and Condensed Fullerane-Like Cages: $\text{Na}_{172}\text{In}_{197}\text{Z}_2$ ( $Z = \text{Ni, Pd, Pt}$ )

Slavi C. Sevov<sup>1</sup> and John D. Corbett

Department of Chemistry and Ames Laboratory,<sup>2</sup> Iowa State University, Ames, Iowa 50011

Received November 7, 1995; in revised form February 26, 1996; accepted February 29, 1996

Ternary compounds  $\text{Na}_{\sim 172}\text{In}_{\sim 197}\text{Z}_2$  with  $Z = \text{Ni, Pd or Pt}$  are obtained by slow cooling of the appropriate fused mixtures of the elements in welded Ta. They occur in the orthorhombic space group  $Pm\bar{m}n$ ,  $Z = 2$  and, for Ni,  $a = 15.988$  (5),  $b = 26.102$  (7),  $c = 47.59$  (6) Å and  $R(\text{F})$ ,  $R_w = 6.0, 6.7\%$  for the refined composition  $\text{Na}_{171.85(5)}\text{In}_{197.1(2)}\text{Ni}_2$ . The structure contains puckered layers of condensed fullerane-type spheres or cages built of 70 and 78 indium atoms, each of which shares six of its twelve pentagonal faces with six other spheres, two of the same type and four of the other. These are joined into double layers via bonds to exo  $\text{In}_{11}$  and  $\text{In}_{14}$  polyhedra fused near one pole of the two fullerenes. The double layers are in turn separated by sodium cations and  $M_{60} = \text{In}_{48}\text{Na}_{12}$  cages which share six of their pentagonal faces with two  $\text{In}_{70}$  cages and four  $\text{In}_{78}$  cages. All three cages have  $C_{2v}$  symmetry but are close to those of the corresponding carbon fullerenes. The  $\text{In}_{70}$  and  $M_{60}$  cages are centered by isolated  $\text{In}_{\sim 10}\text{Z}$  clusters, and the  $\text{In}_{78}$  spheres, by  $\text{In}_{16}$  clusters about a central Na that are tethered to the inside of the  $\text{In}_{78}$  fullerane via vertices of two icosahedra fused into the framework. In addition, all three cages contain endohedral sodium ion deltahedra that screen the encapsulated clusters from the fullerane. The partially disordered Ni-centered clusters of indium exhibit nearly spherical geometry and a diffuse distribution of the electron density on the surface that is excluded from positions below the 12 more inward-lying Na within the corresponding fullerenes. The cluster distributions were approximated by refining many closely positioned indium atoms, some partially occupied. In all three cases, the results could be reduced to geometries close to those of previously known  $\text{In}_{10}\text{Ni}^{10-}$  (within  $\text{In}_{70}$ ,  $M_{60}$ ) or  $\text{In}_{16}$  (within  $\text{In}_{78}$ ) species through removal of the disorder induced by mirror planes from the  $C_{2v}$  symmetry imposed by the overall structure. The multiply endohedral descriptions  $\text{Ni}@\text{In}_{10}@\text{Na}_{37}@\text{In}_{70}$  and  $\text{Ni}@\text{In}_{10}@\text{Na}_{32}@\text{In}_{48}\text{Na}_{12}$  are apt for the first two fullerane components.

<sup>1</sup> Present address: Department of Chemistry and Biochemistry, University of Notre Dame, Notre Dame, IN 46556.

<sup>2</sup> The Ames Laboratory is operated for the U.S. Department of Energy by Iowa State University under Contract W-7405-Eng.-82. This research was supported by the Office of the Basic Energy Sciences, Materials Sciences Division, DOE. The U.S. Government's right to retain a nonexclusive royalty-free license in and to the copyright covering this paper, for governmental purposes, is acknowledged.

The suitability of large polyhedral constructs for the description of other condensed structures is also considered. © 1996 Academic Press, Inc.

## INTRODUCTION

The very active field of fullerene science, including exo- and endohedral derivatives and extensions into macro-spheres and tubes (1–4), pertains almost exclusively to  $\pi$ -bonded carbon frameworks, although the popular and singular appellation “fullerene” is intended to convey more geometric information. We earlier reported a major new solid state variation on this theme in the remarkable structure associated with the isostructural series  $\text{Na}_{96}\text{In}_{97}\text{Z}_2$ , in which  $Z$  may be Ni, Pd or Pt (structures with Ni and Pd were both refined in  $P6_3/mmc$ ) (5). The compound is based on  $\text{In}_{74}$  and  $M_{60} = \text{In}_{48}\text{Na}_{12}$  “buckyballs” as building blocks, and the unusual, even unique features, of the structure that are pertinent to the present article are the following:

1. The  $\text{In}_{74}$  cages, rigorously  $D_{3h}$  in symmetry, are condensed through sharing of the six regularly-disposed pentagonal faces about the waist of each unit to generate layers of close-packed  $\text{In}_{74}$  units. These in turn pack h.c.p.
2. Each  $\text{In}_{74}$  is composed of onion-like layers. Well-defined sodium atom polyhedra lie outside and inside every face of the cage, 39 in number, so that the latter cation cage screens an innermost cluster from the indium cage. This cluster consists of a central Ni (or other  $Z$ ) atom surrounded by close to 10 indium atoms and appears to be similar, even identical, to the isolated  $\sim C_{3v}$  unit  $\text{In}_{10}\text{Ni}^{10-}$  already identified in  $\text{K}_{10}\text{In}_{10}\text{Ni}$  (6). The constituents of the onion can be expressed in terms of the multiply endohedral polyhedra  $\text{Ni}@\text{In}_{10}@\text{Na}_{39}@\text{In}_{74}$ . The innermost cluster is partially disordered, evidently because of the incommensurate symmetries of the  $\text{Na}_{39}$  shell ( $D_{3h}$ ) and the  $\text{In}_{10}\text{Ni}$  core, ( $\sim C_{3v}$ ). The cavity within the  $\text{Na}_{39}$  shell is defined mainly by the 12 more inward-lying sodium atoms that cap the pentagonal faces on  $\text{In}_{74}$ . The X-ray refinement then gives (within the usual centric ellipsoid distribution) pancakes of indium electron density that lie between these Na points

and sum to very close to 10 In per Ni. These clusters are better resolved in the present structure.

3. The need for at least four sigma bonds to each In (lacking any  $\pi$  bonding of significance) means that further modifications of the simple picture of condensed  $\text{In}_{74}$  units are necessary. Atoms adjacent to those in the pentagons shared between two cages also form typical two-center-two-electron bonds. Other atoms nearer the poles of the  $\text{In}_{74}$  cage achieve a fourth bond via additional planar  $\text{In}_6$  and  $\text{In}_3$  “decorations.” Outward pointing lone pairs on the latter apparently define the HOMO states or bands.

4. Spaces between the *hcp* layers of condensed and stuffed  $\text{In}_{74}$  spheres are filled by  $M_{60} = \text{In}_{48}\text{Na}_{12}$  ( $D_{3d}$ ) polyhedra in which the In components come from both pentagons near the poles of six  $\text{In}_{74}$  units and their decorations on the two adjoining augmented layers. This mixed cage also contains a similar disordered  $\text{In}_{10}\text{Ni}$  unit and a sphere of 32 intervening sodium atoms, viz.,  $\text{Ni}@ \text{In}_{10}@\text{Na}_{32}@\text{M}_{60}$ .

Another important aspect of  $\text{Na}_{96}\text{In}_{97}\text{Ni}_2$  is how close this compound is in composition and electron count to the simple  $\text{NaIn}$  obtained without the trace of Ni, a Zintl phase that can be described fairly well as a  $\text{Na}^+$ -stuffed diamond lattice built of  $\text{In}^-$ . The size of sodium seems critical as potassium appears to give instead only  $\text{K}_{10}\text{In}_{10}\text{Z}$  with, similarly,  $Z = \text{Ni}, \text{Pd},$  or  $\text{Pt}$ . We will hereafter follow the suggestion of Nesper (7) that the saturated, although still delocalized, bonding in these buckeyball-like compounds means they are probably better called *fulleranes*.

We report here a second, related compound type for which we have refined the structure for  $Z = \text{Ni}$ . The result is clearly related to the hexagonal  $\text{Na}_{92}\text{In}_{97}\text{Z}_2$  but has both greater complexity (141 rather than 39 independent atoms) and lower orthorhombic symmetry. The fact that all cages now have  $C_{2v}$  symmetry allows a considerably clearer resolution of the disorder of the intermost centered clusters, which are  $\sim \text{In}_{10}\text{Ni}$  units centered in both  $\text{In}_{70}$  ( $\sim D_{3h}$ -I type  $C_{70}$ ) and  $M_{60}$  ( $\text{In}_{48}\text{Na}_{12}$ ) cages and  $\text{In}_{16}(\text{Na})$  in the  $\text{In}_{78}$  fullerane. However, some of the  $\text{In}_5$  pentagons and  $\text{Na}_2$  edges that are shared between these fulleranes in this structure are positioned away from the waists of the cages, and so heterocage condensation produces puckered layers. Augmentation of the  $\text{In}_{70}$  and  $\text{In}_{78}$  cages near their poles by smaller fused indium clusters or added  $\text{In}_3$ ,  $\text{In}_6$  features (very similar to those seen before) serve to interlink or line the layers and again to give all indium four or more like neighbors. The sodium polyhedra that again result from capping of all faces of the fullerane cages inside and out serve to insulate the centered indium–nickel clusters from the indium cages and also to restrict the disorder of the nearly spherical clusters. The complexity of the structure together with the regularities therein are again evidence of a remarkable drive to satisfy the covalent bonding

requirements of indium, to accommodate the necessary cations in alternating anion–cation–anion functions, and to fill space efficiently. At the same time, the size of the structure and the details of the surface augmentation of the layers by additional small indium groups make detailed calculations and electronic understanding out of the question. The lack of quantitative yields has unfortunately precluded measurements of any other physical properties.

Finally, we will also discuss the observations by Nesper (7) that related polyhedral properties can also be found in a few other compounds. However, most of these appear distinctly different in that these cage polyhedra are not of the nature of building blocks, but rather are distributed on the surfaces of larger spheres imposed on the structures, for example, the  $\text{B}_{60}$  polyhedron found on cutting through the linked and condensed icosahedra in  $\beta$ -B (8).

## EXPERIMENTAL SECTION

### Syntheses

All materials were handled in a  $\text{N}_2$ -filled glovebox with a typical  $\text{H}_2\text{O}$  level of less than 0.1 ppm vol. The surfaces of the indium (Cerac, 99.999%) and sodium (Alfa, 99.9+%, sealed under Ar) were cleaned with a scalpel before use. Nickel sheet (Matheson, Coleman & Bell, reagent), palladium wire (Johnson-Matthey, 99.995%) and platinum sheet (Government issue, reagent) were used as received. All reactions were carried out in welded tantalum tubes jacketed in sealed silica containers, techniques that are described elsewhere (9).

Initially the phase  $\text{Na}_{\sim 172}\text{In}_{\sim 197}\text{Ni}_2$ , hereafter denoted **II**, was distinguished by the specific barlike shape of the crystals in the product of a reaction loaded as  $\text{Na}_{10}\text{In}_{10}\text{Ni}$ , heated at  $600^\circ\text{C}$ , and cooled at  $5^\circ \text{hr}^{-1}$ . After its structure had been partially refined and the approximate composition determined, samples with an atomic ratio of  $\text{Na}:\text{In}:\text{Ni}, \text{Pd}$  or  $\text{Pt} = 174:194:2$  were prepared, melted at  $700^\circ\text{C}$  for one day (the highest melting point in the  $\text{Na}$ – $\text{In}$  system is about  $440^\circ\text{C}$ ), and then slowly cooled to room temperature at  $5^\circ \text{hr}^{-1}$ . Although **II** forms barlike crystals with Ni, those with Pd or Pt are instead needle-like. All have a dark gray color and metallic luster. The crystals of **II** can be distinguished easily from the bar-like crystals of **I**,  $\text{Na}_{96}\text{In}_{97}\text{Z}_2$ , by the direction of the striations that can be seen on the faces of the crystals with a conventional optical microscope. In **I**, these run perpendicular to the bar direction (the  $c$  axis of the hexagonal unit cell, which is normal to the layers of fused  $\text{In}_{74}$ ) while the striations on **II** are parallel to the bar length, which lies along the short  $a$  axis, and thus may also be normal to the longest axis ( $c$ ) and parallel to the layers of  $\text{In}_{70}$  and  $\text{In}_{78}$ . The acicular crystals of the isostructural Pd and Pt derivatives of **II** are of course very easily distinguished from the rest.

Unfortunately, reactions loaded close to the stoichiome-

try of **II-Z** did not provide a high yield of any of these, rather giving 60–70% yields at best. Probably the compounds melt incongruently, and slow cooling leads to formation of other phases as well. Quenching and subsequent annealing at proper temperature could provide better yields. Another difficulty encountered with the characterization of **II**-type phases was that their powder pattern lines could not be sorted out in the presence of **I** because the respective *a* and *c* lattice parameters of the two types are very close to each other, and many of the diffraction lines overlap. Moreover, the strongest line of phase **II** falls at an extremely low  $2\theta$  value where it is buried in the high film background in this region. The rest of the lines are so weak (the next strongest is about 15/100) and so close to each other that they can hardly be identified in the presence of other phases. These features make visual phase identification on the basis of morphology the easier approach.

X-ray powder patterns were obtained from ground samples that were mounted between pieces of cellophane tape. An Enraf–Nonius Guinier camera,  $\text{CuK}\alpha_1$  radiation ( $\lambda = 1.540562 \text{ \AA}$ ), and NIST silicon as an internal standard were employed for this purpose. All powder patterns of **II–Z** also contained lines from the corresponding **I**,  $\text{NaIn}$  and  $\text{In}$ ; in addition, products of reactions loaded as  $\text{Na}_{10}\text{In}_{10}\text{Z}$  ( $Z = \text{Ni, Pd, Pt}$ ) also appeared to contain lines from possibly related, although not identical, isolated cluster phases  $\text{Na}_{10}\text{In}_{10}\text{Z}$ ; that is, some matched those calculated on the basis of the known  $\text{K}_{10}\text{Ni}_{10}\text{Z}$ . Since the lines could not be well distinguished, as discussed above, neither the lattice parameters nor the reaction yields were determined from representative samples by powder diffraction. The reaction yields were deduced from the characteristic morphologies, while the lattice parameters of **II** were determined from patterns of selectively collected and ground crystals. However, even these patterns displayed sections with nearly continuous intensity which on the calculated powder pattern appeared as groups of many lines with nearly equal angles and intensities. Assignment of the correct Miller indices to most (on the basis of the refined structure) was practically impossible. Only 21 lines could be assigned with relatively great certainty, and a least-squares refinement of the measured  $2\theta$  values of these, together with those of the standard Si lines resulted in  $a = 15.988(5)$ ,  $b = 26.102(7)$  and  $c = 47.59(6) \text{ \AA}$ . These are considered to be more accurate than those determined on the diffractometer because of alignment uncertainties.

### Structure Determination

Diffraction data for **II** were collected on a CAD4 single crystal diffractometer. Several bar-like crystals from a sample loaded as  $\text{Na}_{10}\text{In}_{10}\text{Ni}$  were sealed in thin-walled capillaries and checked for singularity by means of oscillation photographs. One of them,  $0.15 \times 0.2 \times 0.3 \text{ mm}$ , was

TABLE 1  
Data Collection and Refinement Parameters for  
 $\text{Na}_{171.85(5)}\text{In}_{197.1(2)}\text{Ni}_2$

Formula weight	26705
Crystal size, mm	$0.15 \times 0.20 \times 0.30$
Lattice parameters: <sup>a</sup>	
<i>a</i> , $\text{\AA}$	15.988(5)
<i>b</i> , $\text{\AA}$	26.102(7)
<i>c</i> , $\text{\AA}$	47.59(6)
<i>V</i> , $\text{\AA}^3$	19860(36)
Space group, <i>Z</i>	<i>Pmnm</i> (No. 59), 2
<i>d</i> (calc.), $\text{g cm}^{-3}$	4.46
$\mu(\text{MoK}\alpha)$ , $\text{cm}^{-1}$	113.12
Normalized transmission range	0.6742–1.00
Diffractometer, radiation	CAD4, $\text{MoK}\alpha$
Temperature, $^\circ\text{C}$	23
Octant measured	<i>h, k, l</i>
Scan method	$\omega$
$2\theta_{\text{max}}$	$50^\circ$
Number of reflections:	
indep. measured	18822
indep. observed ( $I \geq 3\sigma_I$ )	8120
Number of variables	1000
<i>R</i> ; <i>R<sub>w</sub></i> , % <sup>b</sup>	6.0; 6.7
Goodness-of-fit indicator	1.62
Maximum shift/ $\sigma$ in final cycle	0.03
Largest peaks in final $\Delta F$ map	$+5.3 e/\text{\AA}^3$ (0.45 $\text{\AA}$ from $\text{Na30}$ ), $-4.1 e/\text{\AA}^3$
Secondary ext. coeff.	$1.2(2) \times 10^{-9}$

<sup>a</sup> Room temperature Guinier data with Si as an internal standard ( $\lambda = 1.540562 \text{ \AA}$ ).

<sup>b</sup>  $R = \sum ||F_o| - |F_c|| / \sum |F_o|$ ;  $R_w = [\sum w(|F_o| - |F_c|)^2 / \sum w(F_o)^2]^{1/2}$ ;  $w = \sigma_F^{-2}$ .

mounted on the diffractometer, and 25 reflections were found from a random search indexed with a primitive orthorhombic unit cell. Data collected at  $23^\circ\text{C}$  with monochromated  $\text{MoK}\alpha$  radiation for one octant of reciprocal space up to  $2\theta = 50^\circ$  were corrected for Lorentz and polarization effects and for absorption with the aid of the average of five  $\Psi$ -scans at different  $2\theta$  angles. The observed absence condition for  $hk0$ ,  $h + k \neq 2n$ , suggested three possible space groups:  $Pm2_1n$ ,  $P2_1mn$ , and  $Pmnm$ . The Wilson plot corresponded to a centrosymmetric distribution and therefore  $Pmnm$  was chosen. The reflections were very sharp (*ca.*  $0.4^\circ$  wide in  $\omega$ ) and, although the *c* axis is quite long, the programmed  $\omega$ - $\theta$  scans demonstrated that no overlap of reflections occurred when data collection was done with  $0.4^\circ$ -wide  $\omega$ -scans and a vertical detector slit equivalent to  $0.82^\circ$ .

The structure was refined with the aid of the TEXSAN software package. Some details of the data collection and refinement are listed in Table 1. Direct methods (SHELXS-86) (10) provided 57 unique peaks that had distances to each other appropriate for indium atoms, and

they were so assigned. A few cycles of least-squares refinement and a difference Fourier synthesis revealed two atoms at special positions with many peaks surrounding them at distances appropriate for Ni–In distances and also many other positions with distances to In appropriate for sodium. After assignment of the first two positions to Ni atoms and the latter to Na atoms, subsequent refinement and difference Fourier map revealed a few more Na atoms, but the electron density shell around the two independent Ni atoms remained. The peaks in these shells were of relatively low heights, and some of them were too close to each other, although all of them had distances to the central atom appropriate for In–Ni. All 68 sodium atoms were located by repeating the sequence of least-squares refinement, difference Fourier synthesis, and addition of new atoms. At this point, almost all indium atoms from the fused cages (In1 to In52, but not In53) and some of those in the cluster within In<sub>78</sub> (InC1 to InC5) had been located and refined. But In52, InC3–InC5, and Na37 had abnormally large thermal parameters, Na1 had a negative thermal parameter, and the previously noted electron density areas of relatively low height (*ca.* 20 to 30 e/Å<sup>3</sup>) remained present around the two nickel positions as well as near InC3, C4 and C5. A few of these maxima were assigned as indium, and a subsequent least-squares refinement led to unusually high thermal parameters for them. A similar situation had already been encountered for Na<sub>96</sub>In<sub>97</sub>Ni<sub>2</sub> (5).

At this point, the well behaved indium atoms were refined with anisotropic thermal parameters, and In52 and the group InC(3, 4, 5) were refined with partial occupancies. This gave an *R* of around 15%. Next, all of the peaks remaining around the Ni atoms and those near InC(3,4,5) were input as In atoms and their anisotropic thermal parameters as well as their occupancies were eventually refined. All sodium atoms were refined anisotropically as well. This led to non-positive-definite parameters for Na1, 3, 30, 37, and 51, and so they were held to isotropic variations. The *R*(*F*) and *R*<sub>w</sub> factors at this point had dropped to 6.3 and 7.0%, respectively. A large positive peak of about 10 e/Å<sup>3</sup> remained in the difference Fourier map about 1.4 Å from Na37 (the sodium atom with relatively large thermal parameter) and about 2.8 Å from In19, 40, 43, and it was paired with a symmetry-equivalent position generated by a mirror plane through Na37. A Fourier map calculated from *F*<sub>obs</sub> clearly showed a nearly spherical “island” of electron density at each of the two symmetry-related positions. More careful study of their environment revealed that they were parts of two otherwise *arachno* indium icosahedra fused to the cages (see Structure Description). The two problem positions, if filled, would connect what become two *nido* icosahedra and would also be a part of an In<sub>78</sub> fullerane-type cage and make it a *closo*-type. Distances of each of the pair to the surrounding

indium atoms were more appropriate for indium atoms, and so In53 was refined there with partial occupancy and the multiplicity of Na37 was also freed. This resulted in 85(5)% occupancy of Na37 site and two 30(2)%-occupied In53 sites. The sum of the two occupancies, 115(5)%, falls within 3σ of 100% and suggests to us that the two nearby sites of In53 are occupied when Na37 is not present.

Na1 remained with a negative thermal parameter but within 1σ of zero in the final refinement. It centers a roughly 16-atom (possibly defect) indium deltahedron built of InC1–C7 with distances from Na1 that range from 3.23 to 3.52 Å. Such large distances exclude the possibility of In or Ni as the central atom but are reasonable for Na–In. Moreover, sodium atoms at the center of other relatively large clusters such as 15-bonded *closo*-In<sub>15</sub> in a Na–In–Au compound (11), 8- and 12-bonded *closo*-In<sub>16</sub> in Na<sub>7</sub>In<sub>11.8</sub> (9) and Na<sub>15</sub>In<sub>27.4</sub> (12), respectively, 12-bonded *closo*-In<sub>18</sub> in a Na–In–Sn compound (11), and *closo*-Tl<sub>12</sub> in Na<sub>15</sub>K<sub>6</sub>Tl<sub>18</sub>H (13) are always found to have relatively small thermal parameters. Another reason why this particular sodium atom refines with a (slightly) negative thermal parameter may come from the fact that the surrounding InC3–C7 atoms all refined with 50–88% occupancies and InC6 and C7 among these have extremely anisotropic thermal parameters.

The occupancy of In52 is 59(1)% in the final refinement. This atom is 6-bonded within a *nido* In<sub>14</sub> cluster that is fused to the surface of In<sub>70</sub> (see Structure Description) and would, if fully occupied, have an additional exo bond to its symmetry-related counterpart. This would seem to be unfavorable according to our experiences with Na<sub>15</sub>In<sub>27.4</sub> (12) and other phases with similarly positioned atoms (11). Usually, In atoms with seven possible neighbors occur at close to half occupancy, as in this case, so that when one position is occupied its symmetry-related counterpart is evidently empty, and formation of the corresponding, generally unfavorable seventh exo bond between the two atoms is avoided.

After all of the foregoing (some of which will receive further clarification later), the final residuals were *R*, *R*<sub>w</sub> = 6.0, 6.7%, respectively, and the largest residual peaks in the final difference Fourier map were 5.3 e/Å<sup>3</sup>, 0.45 Å from Na30 (refined only isotropically, endohedral to In<sub>78</sub>), and –4.1 e/Å<sup>3</sup>. The total numbers of In atom neighbors around NiA, NiB, and Na1 summed to 10.0 (2), 10.08 (7), and 14.4 (1), respectively, when the single anisotropic ellipsoidal description of each site was presumed to give a good representation of the total In present. This led to the final refined composition Na<sub>171.85(5)</sub>In<sub>197.1(2)</sub>Ni<sub>2</sub> for the independent unit.

Since the electron density distributions around NiA, NiB, and, partially, around Na1 were at this stage approximated as many closely positioned, partially occupied and quite anisotropic (pancake-shaped) indium atoms, a rea-

sonable question arises about the correctness of the chosen space group. Clearly, many of the indium atoms around NiA and, to some extent, those around NiB and Na1 are too close to each other, which, we believe, originates from mirror planes that pass through the central atoms (all are  $C_{2v}$  according to the space group). Although those mirror planes appear to be artificial for these clusters (below), they are definitely there for the rest of the atoms, and these account for about 88% of the scattering power (130 atoms out of the total of 141). From our experience with the similar behavior of the isolated clusters in  $\text{Na}_{96}\text{In}_{97}\text{Ni}_2$ , we concluded that a larger set of data and subsequent refinement in a lower symmetry space group would not eliminate the problem. (Reduction of the symmetry from  $P6_3/mmc$  all the way to  $P2_1$  did not lead to better results for  $\text{Na}_{96}\text{In}_{97}(\text{Ni or Pd})_2$ .) The large number of atoms that *have* the symmetry elements of the chosen space group will generate structure factors that are practically the same in any subgroup. In other words, the contribution from atoms that may not reflect some of the symmetry elements is so small that, although the real space group may be of lower symmetry, refinement in it is practically impossible. As a matter of fact, our conclusions about the NiA and NiB examples (later) is that the inner  $\text{NiIn}_{-10}$  units are truly disordered, for good reason.

Data were later collected on a second less well-shaped crystal ( $\sim 0.1 \times 0.2 \times 0.2$  mm) of **II**, but it diffracted more weakly than the first crystal (6951 rather than 8120 observed reflections), and this led to about  $\sim 50\%$  larger standard deviations in the final refined parameters. The structure refined to  $R/R_w = 6.4, 7.2\%$  (GOF = 1.68, 960 (vs 1000) variables, largest peaks in  $\Delta F = +5.1$  and  $-3.8$   $e/\text{\AA}^3$ , normalized transmission coefficient range 0.598–1.000), and the resultant composition was  $\text{Na}_{171.8(1)}\text{In}_{197.5(3)}\text{Ni}_2$ , within 1  $\sigma$  of that previously obtained. All atoms except Na3, 5, 8, 17, 19, 21, 23, 37, 39, 45, 51, 52, 60, 62, and 63 and In53 could be refined with anisotropic thermal parameters, the parameters for these becoming non-positive-definite when so treated. The final thermal parameter for Na1 was slightly negative ( $-0.2(4)$   $\text{\AA}^2$ ), as for the first crystal. The indium atoms forming the isolated clusters around the nickel atoms and some of those around Na1 again had very anisotropic, nearly two-dimensional thermal ellipsoids. The occupancies of all of the sites in the encapsulated indium clusters were within  $3\sigma$  of those refined for the first crystal. Also, In52 refined with 54(1)%, In53 with 17(1)%, and Na37 with 84(7)% occupancies, supporting the idea that these are intrinsic characteristics of the structure.

## RESULTS AND DISCUSSION

The final positional and isotropic-equivalent displacement parameters for  $\text{Na}_{171.85(5)}\text{In}_{192.1(2)}\text{Ni}_2$  as well as data

on the partially occupied sites are reported in Table 2. The anisotropic displacement parameters and other data are available from the authors. Virtually all of the figures are drawn with the refined ellipsoid values. Important distances out to 4.00  $\text{\AA}$  about all atoms are listed in Table 3. These show that the polyhedra of In about both In and Na are well defined and closed well below the cutoff.

### The Cage Components of the Structure

A structure of this complexity requires substantial development. The construction can be viewed in two ways. In the first, only bonding between the indium atoms is considered; in the second, sodium atoms are added to the description. For the first, an overview of the character of the unit cell contents is shown in Fig. 1 in which the  $\text{In}_{70}$  (A) and  $\text{In}_{78}$  (C) cages that form mixed layers are represented only as spheres while lines drawn between indium atoms between pairs of layers mark all separations less than 4.0  $\text{\AA}$ . The structure is built of puckered double layers perpendicular to the  $c$  axis (vertical) that lie around  $z = 0.5$  while gaps between the double layers fall at  $z = 0$  and 1. Thus, there is no direct In–In bonding between the double layers. The individual layers have quasi close-packed arrangements of face-sharing  $\text{In}_{70}$  and  $\text{In}_{78}$  cages. The sequence of these cages is such that rows of each type run along the  $a$  axis (nearly the view direction in Fig. 1) while the cage types alternate along the  $b$  axis (horizontal) to give a puckered or wave-like sequence in this direction. Two such layers are bonded together to generate the double layer (around  $z = 1/2$ ) through quite complicated In–In bonding. Some of the atoms in the cage layers about  $z = 0$  also have approximately outward pointing exo bonding to other “surface” indium atoms that do not belong to a cage and do not interconnect cages.

Figure 2 shows the 70 indium atoms of cage **A** with the unique atoms labeled. This has  $C_{2v}$  point symmetry (the 2-fold axis is vertical in the figure, and the two mirror planes are nearly in and normal to the page), but the cage is very close to  $D_{5h}$ , the symmetry of the  $C_{70}$  fullerene (the pseudo 5-fold axis lies nearly along the view direction). All atoms exhibit small, well behaved ellipsoids (those for 30% probability are shown). The two pentagons generated by In1, 34, and 50 and the consequences of a mirror plane are shared with two other  $\text{In}_{70}$  cages in the string along the  $a$  axis. The four pentagonal faces near the waist that are composed of In9, 27, 36, 44, and 47 are shared with four separate  $\text{In}_{78}$  cages, while the two hexagonal faces near the top, In16, 29, 31, and 45, are also parts of *nido*- $\text{In}_{14}$  clusters (not shown) to be discussed later. (This and succeeding figures show In–In connections for all separations listed in Table 3. There is more than a 0.6  $\text{\AA}$  gap beyond these, so the bonding polyhedra are quite clearly defined.)

TABLE 2  
 Positional and Isotropic Equivalent Displacement Parameters for  $\text{Na}_{171.85(5)}\text{In}_{197.1(2)}\text{Ni}_2$

Atom	N	x	y	z	$B_{\text{eq}}$	Occup.	No. at./clust.
In1	2b	3/4	1/4	0.26040(9)	1.4(2)		
In2	4f	0.3443(2)	3/4	0.11108(6)	1.6(1)		
In3	8g	0.4369(1)	0.65645(9)	0.09142(4)	1.4(1)		
In4	4f	0.3448(2)	3/4	0.51146(6)	1.3(1)		
In5	4e	1/4	0.6581(1)	0.20301(6)	1.5(1)		
In6	8g	0.6548(1)	0.4373(1)	0.17040(4)	1.34(9)		
In7	4e	1/4	0.5385(1)	0.32785(6)	1.5(1)		
In8	8g	0.4400(1)	0.4654(1)	0.08901(4)	1.5(1)		
In9	8g	0.6556(1)	0.4379(1)	0.27854(4)	1.36(9)		
In10	8g	0.5576(1)	0.34286(9)	0.18883(4)	1.4(1)		
In11	4e	1/4	0.4663(1)	0.20202(7)	1.5(1)		
In12	8g	0.4397(1)	0.5623(1)	0.12826(4)	1.47(9)		
In13	8g	0.4148(1)	0.6944(1)	0.35840(4)	1.5(1)		
In14	4f	0.4141(2)	3/4	0.45390(6)	1.4(1)		
In15	8g	0.3466(1)	0.63719(9)	0.30998(4)	1.4(1)		
In16	4e	1/4	0.5025(1)	0.38973(6)	1.4(1)		
In17	2b	1/4	3/4	0.1666(1)	1.7(2)		
In18	8g	0.3453(1)	0.5599(1)	0.07085(4)	1.6(1)		
In19	4f	0.5847(2)	3/4	0.34852(7)	1.9(1)		
In20	8g	0.4133(1)	0.65989(9)	0.41703(4)	1.4(1)		
In21	8g	0.4044(1)	0.30830(9)	0.15867(4)	1.3(1)		
In22	4e	3/4	0.5325(1)	0.09087(6)	1.5(1)		
In23	8g	0.5888(1)	0.69289(9)	0.06053(4)	1.5(1)		
In24	8g	0.5627(1)	0.46102(9)	0.38271(4)	1.31(9)		
In25	8g	0.6553(1)	0.36602(9)	0.39894(4)	1.34(9)		
In26	4e	1/4	0.5598(1)	0.49237(6)	1.9(1)		
In27	8g	0.5624(1)	0.4979(1)	0.32145(4)	1.4(1)		
In28	8g	0.5957(1)	0.4984(1)	0.12171(4)	1.5(1)		
In29	8g	0.4106(1)	0.4610(1)	0.41652(4)	1.5(1)		
In30	4f	0.6543(2)	1/4	0.20652(6)	1.3(1)		
In31	8g	0.4105(1)	0.36757(9)	0.45389(4)	1.5(1)		
In32	4e	1/4	0.3728(1)	0.16407(6)	1.4(1)		
In33	4e	1/4	0.4673(1)	0.52916(6)	2.0(2)		
In34	4e	3/4	0.3418(1)	0.29589(6)	1.5(1)		
In35	8g	0.3445(1)	0.3684(1)	0.10680(4)	1.6(1)		
In36	8g	0.4094(1)	0.5342(1)	0.29340(4)	1.5(1)		
In37	8g	0.3463(1)	0.5636(1)	0.18350(4)	1.6(1)		
In38	8g	0.3450(1)	0.36979(9)	0.51270(4)	1.5(1)		
In39	8g	0.3449(1)	0.5621(1)	0.43639(4)	1.6(1)		
In40	8g	0.5844(1)	0.65772(9)	0.38386(4)	1.6(1)		
In41	8g	0.6546(1)	0.5580(1)	0.36605(4)	1.5(1)		
In42	8g	0.4367(1)	0.69103(9)	0.55649(4)	1.4(1)		
In43	8g	0.5843(1)	0.69348(9)	0.44227(4)	1.5(1)		
In44	8g	0.4088(1)	0.4987(1)	0.23248(4)	1.5(1)		
In45	4e	1/4	0.3084(1)	0.46672(6)	1.5(1)		
In46	4e	1/4	0.6936(1)	0.26430(7)	1.7(1)		
In47	8g	0.5612(1)	0.4389(1)	0.22441(4)	1.35(9)		
In48	8g	0.6522(2)	0.6340(1)	0.00691(4)	1.8(1)		
In49	4e	3/4	0.6361(1)	0.06511(6)	1.3(1)		
In50	4e	3/4	0.3065(1)	0.35420(6)	1.3(1)		
In51	4e	3/4	0.5380(1)	0.02541(7)	1.7(1)		
In52	8g	0.4155(3)	0.4825(2)	0.48714(9)	2.7(2)		
In53	4f	0.665(1)	3/4	0.3997(4)	2.0(10)	30(2)%	

(continued)

TABLE 2—Continued

Atom	N	x	y	z	$B_{eq}$	Occup.	No. at./clust.
NiA	2a	1/4	1/4	0.3114(1)	0.8(3)		
InA1	8g	0.2198(5)	0.1530(2)	0.3290(1)	6.5(5)	50(1)%	2.00(4)
InA2	4f	0.3759(8)	1/4	0.3505(3)	10.2(9)	50(4)%	1.00(8)
InA3	8g	0.1075(6)	0.1883(4)	0.3165(3)	11.5(7)	50(2)%	2.00(8)
InA4	8g	0.1083(5)	0.2084(4)	0.2879(2)	8.5(5)	50(2)%	2.00(8)
InA5	4f	0.196(1)	1/4	0.3647(2)	8.8(7)	50(4)%	1.00(8)
InA6	8g	0.2224(6)	0.1924(3)	0.2652(1)	7.6(5)	50(1)%	2.00(4)
						total	10.0(2)
NiB	2b	3/4	1/4	0.0492(1)	1.0(3)		
InB1	8g	0.6576(3)	0.1936(2)	0.0847(1)	10.7(3)	100(1)%	4.00(4)
InB2	2b	3/4	1/4	0.9937(1)	13.2(8)	100(1)%	1.00(1)
InB3	8g	0.7062(8)	0.1558(3)	0.0349(3)	19.0(10)	57(1)%	2.28(4)
InB4	8g	0.634(1)	0.1932(7)	0.0235(3)	14.0(10)	35(1)%	1.40(4)
InB5	4f	0.5901(5)	1/4	0.0310(2)	8.8(6)	70(1)%	1.4(2)
						total	10.08(7)
InC1	4f	0.6559(3)	3/4	0.29277(8)	3.4(2)	100(1)%	2.00(2)
InC2	4e	3/4	0.6497(2)	0.2738(1)	4.0(2)	100(1)%	2.00(2)
InC3	8g	0.0826(2)	0.1864(2)	0.75463(9)	7.5(2)	88(1)%	3.52(4)
InC4	4e	1/4	0.1210(3)	0.7853(1)	15.0(7)	86(2)%	1.72(4)
InC5	4e	1/4	0.1963(4)	0.8364(1)	18.0(8)	78(2)%	1.56(4)
InC6	4f	0.0801(5)	1/4	0.8109(1)	23.0(10)	80(1)%	1.60(2)
InC7	8g	0.1263(9)	0.1640(8)	0.8109(3)	27.0(10)	50(1)%	2.00(4)
						total	14.4(1)
Na1	2a	1/4	1/4	0.7740(4)	-0.2(3)		
Na2	4e	1/4	0.4452(7)	0.4579(3)	2.0(8)		
Na3	4e	3/4	0.4408(7)	0.3453(3)	2.0(3)		
Na4	4f	0.563(1)	3/4	0.5073(3)	3.0(10)		
Na5	2a	1/4	1/4	0.1969(5)	2.0(10)		
Na6	2a	1/4	1/4	0.1226(5)	3.0(10)		
Na7	8g	0.5946(8)	0.0615(5)	0.4533(3)	2.6(6)		
Na8	2b	3/4	1/4	0.4195(5)	2.0(10)		
Na9	4e	3/4	0.1307(9)	0.8712(4)	3.0(10)		
Na10	4e	3/4	0.0186(7)	0.4119(3)	2.1(8)		
Na11	8g	0.0574(8)	0.0611(5)	0.5673(2)	2.2(5)		
Na12	4e	1/4	0.1848(7)	0.0504(4)	2.5(9)		
Na13	4f	0.126(1)	1/4	0.4215(4)	3.0(10)		
Na14	8g	0.5757(8)	0.1761(5)	0.2560(2)	2.5(6)		
Na15	4f	0.560(1)	1/4	0.7081(4)	4.0(10)		
Na16	4e	1/4	0.0448(6)	0.6945(3)	1.7(8)		
Na17	4e	1/4	0.0497(8)	0.8394(4)	3.0(10)		
Na18	4e	1/4	0.0093(8)	0.1272(4)	2.3(9)		
Na19	4e	3/4	0.0036(8)	0.2238(4)	3.0(10)		
Na20	8g	0.1294(8)	0.1291(5)	0.2203(2)	2.7(6)		
Na21	4e	3/4	0.1775(7)	0.1572(4)	1.7(8)		
Na22	8g	0.5442(8)	0.1277(6)	0.1210(2)	2.7(6)		
Na23	4e	3/4	0.1275(7)	0.6213(3)	1.6(3)		
Na24	8g	0.0619(8)	0.0653(6)	0.9381(3)	3.2(7)		
Na25	4e	1/4	0.1187(7)	0.5785(4)	3.0(10)		
Na26	4f	0.052(1)	1/4	0.8767(3)	3.0(10)		
Na27	4e	3/4	0.1735(7)	0.9395(4)	2.2(8)		
Na28	4e	3/4	0.0877(7)	0.1099(3)	2.0(8)		
Na29	4f	0.054(1)	1/4	0.2211(4)	2.1(8)		

TABLE 2—Continued

Atom	N	x	y	z	$B_{eq}$	Occup.	No. at./clust.
Na30	2b	3/4	1/4	0.6666	5.0(8)		
Na31	4e	1/4	0.057(1)	0.2770(4)	4.0(10)		
Na32	2a	1/4	1/4	0.5282(5)	2.0(10)		
Na33	8g	0.1265(7)	0.0553(6)	0.3451(2)	2.6(6)		
Na34	4e	3/4	0.0664(8)	0.7464(3)	2.3(9)		
Na35	4f	0.588(1)	1/4	0.9549(4)	3.0(10)		
Na36	4e	1/4	0.1311(8)	0.4009(4)	3.0(10)		
Na37	2a	3/4	3/4	0.3994(6)	1.8(7)	85(5)%	
Na38	4f	0.605(1)	1/4	0.7787(3)	3.0(10)		
Na39	2b	3/4	1/4	0.5967(6)	4.0(20)		
Na40	8g	0.0461(8)	0.1496(5)	0.3868(3)	2.7(6)		
Na41	8g	0.0882(9)	0.0551(6)	0.7429(3)	3.5(7)		
Na42	8g	0.0665(9)	0.0535(6)	0.1636(2)	3.3(7)		
Na43	4f	0.051(1)	1/4	0.0924(4)	3.0(10)		
Na44	8g	0.5785(8)	0.1268(5)	0.7579(3)	3.0(7)		
Na45	4f	0.605(1)	1/4	0.3131(4)	3.0(10)		
Na46	8g	0.0353(8)	0.1415(5)	0.0504(3)	3.0(6)		
Na47	4e	3/4	0.1476(7)	0.4630(4)	2.1(8)		
Na48	8g	0.088(1)	0.0211(5)	0.0192(2)	3.1(7)		
Na49	8g	0.5559(8)	0.1348(5)	0.5102(2)	2.4(6)		
Na50	4f	0.577(1)	1/4	0.3815(3)	1.8(8)		
Na51	2a	1/4	1/4	0.8997(6)	2.9(6)		
Na52	8g	0.5594(8)	0.0634(6)	0.6327(2)	2.5(6)		
Na53	4f	0.581(1)	1/4	0.1435(4)	3.0(10)		
Na54	8g	0.0490(9)	0.0855(5)	0.2824(2)	2.8(6)		
Na55	4e	1/4	0.055(1)	0.0585(4)	5.0(10)		
Na56	8g	0.1258(9)	0.1286(5)	0.8778(3)	3.0(7)		
Na57	4e	3/4	0.1721(7)	0.5380(4)	2.5(9)		
Na58	8g	0.6315(8)	0.0555(6)	0.0551(2)	3.4(7)		
Na59	4e	3/4	0.1336(9)	0.2236(4)	3.0(10)		
Na60	4e	1/4	0.1707(9)	0.6574(3)	3.0(10)		
Na61	2a	1/4	1/4	0.9718(6)	3.0(10)		
Na62	8g	0.5766(8)	0.1296(6)	0.3323(2)	2.8(6)		
Na63	8g	0.0514(9)	0.0540(7)	0.8132(2)	4.2(7)		
Na64	8g	0.557(1)	0.1327(6)	0.9806(2)	3.9(7)		
Na65	8g	0.0569(9)	0.1321(5)	0.6868(2)	3.0(6)		
Na66	4f	0.073(1)	1/4	0.0050(4)	4.0(10)		
Na67	4e	3/4	0.0693(9)	0.9903(4)	3.0(10)		
Na68	8g	0.571(1)	0.1736(6)	0.8361(3)	3.7(8)		

The more complex and novel  $\text{In}_{78}$  cage (cage **C**) is shown in Fig. 3 with all unique atoms labeled. This sphere also has  $C_{2v}$  point group symmetry (the axis is vertical), but it is very close to  $D_{3h}$  when the appendages at the bottom are neglected. Its geometry can be compared with those predicted for some isomers of  $C_{78}$ . The latter has five allowed isomers according to the isolated-pentagon rule (each pentagon is surrounded only by hexagons),  $C_{2v}$ -I,  $C_{2v}$ -II,  $D_3$ ,  $D_{3h}$ -I and  $D_{3h}$ -II (14), with similar energies, and different authors have predicted different orders of stability based on different calculational methods. Fowler, *et al.* (14) predicted  $D_{3h}$ -II to be the most stable isomer based on the largest HOMO–LUMO gap. The same approach combined with the  $\pi$  resonance energies of the systems gave  $D_{3h}$ -II and  $C_{2v}$ -II as the more stable isomers

(15). Tight-binding molecular dynamics by Ho and co-workers (16) predicted the order of stability  $C_{2v}$ -I >  $D_{3h}$ -I >  $C_{2v}$ -II >  $D_3$  >  $D_{3h}$ -II and, finally, both Diederich *et al.* (17) from force field calculations and Colt and Scuseria (18) from an *ab initio* study gave the order of stability as  $C_{2v}$ -I >  $C_{2v}$ -II >  $D_3$  >  $D_{3h}$ -I >  $D_{3h}$ -II. Experimental NMR studies on  $C_{78}$  fullerenes isolated by chromatography have also produced different results, viz.,  $C_{2v}$ -II and  $D_3$  in the ratio 5:1 (17) or  $C_{2v}$ -I,  $C_{2v}$ -II and  $D_3$  in a ratio 5:2:2 (19). In our case,  $\text{In}_{78}$  (with the constraints provided by condensation) has the geometry of the  $D_{3h}$ -I isomer with the symmetry slightly reduced to  $C_{2v}$ . (The  $C_{2v}$  crystallographic symmetry found here is only coincidental with the symmetry of the first two isomers listed for  $C_{78}$  and results from removal of the 3-fold axis in the isomer  $D_{3h}$ -I without any



**TABLE 3**  
**Distances to Nearest Neighbors about Each Atom in Na<sub>-172</sub>In<sub>-197</sub>Ni<sub>2</sub> ( $d \leq 4.00 \text{ \AA}$ )**

<b>In1</b>		<b>In7</b>		<b>In12</b>		<b>In17</b>		<b>In22</b>		<b>In27</b>	
2	In30 2.986(6)	2	In15 3.121(4)	In3	3.019(3)	2	In2 3.041(6)	2	In28 3.006(3)	In9	2.974(3)
2	In34 2.932(4)		In16 3.092(5)	In8	3.143(4)	2	In5 2.961(4)		In49 2.971(5)	In24	3.070(4)
4	Na14 3.40(1)	2	In36 3.033(3)	In18	3.122(4)				In51 3.119(6)	In36	2.943(3)
2	Na45 3.42(2)		Na23 3.35(2)	In28	3.017(3)	2	Na9 3.59(2)		Na17 3.35(2)	In41	3.024(4)
2	Na59 3.51(2)		Na31 3.47(2)	In37	3.024(4)	2	Na38 3.49(2)		Na24 3.42(1)	Na3	3.53(1)
	<b>In2</b>	2	Na33 3.25(1)	Na9	3.52(1)	4	Na68 3.49(1)	2	Na28 3.26(2)	Na16	3.328(7)
	In2 3.016(7)		Na34 3.61(2)	Na18	3.56(1)		<b>In18</b>		Na56 3.53(1)	Na33	3.51(1)
2	In3 3.005(3)	2	Na52 3.64(1)	Na24	3.71(1)		In3 3.074(3)	2	Na58 3.43(1)	Na41	3.43(1)
	In17 3.041(6)		<b>In8</b>	Na42	3.46(1)		In8 3.020(3)		<b>In23</b>	Na52	3.39(1)
2	Na9 3.56(2)		In12 3.143(4)	Na56	3.45(1)		In12 3.122(4)		In3 2.994(3)	Na54	3.37(1)
	Na26 3.37(2)		In18 3.020(3)	Na63	3.32(1)		In18 3.047(5)		In23 2.981(5)	Na62	3.37(1)
2	Na27 3.47(2)		In28 3.059(3)	Na68	3.37(1)		Na9 3.65(2)		In48 3.146(4)	Na65	3.53(1)
	Na35 3.32(2)		In35 3.077(3)		<b>In13</b>		Na18 3.57(2)		In49 2.980(3)		<b>In28</b>
2	Na68 3.49(2)		Na18 3.60(1)		In13 2.903(4)		Na24 3.49(1)		Na24 3.36(1)	In6	2.967(4)
	<b>In3</b>		Na22 3.32(1)		In15 2.954(4)		Na27 3.37(2)		Na26 3.39(1)	In8	3.059(3)
	In2 3.005(3)		Na24 3.50(1)		In19 3.116(4)		Na48 3.41(1)		Na35 3.28(2)	In12	3.017(3)
	In12 3.019(3)		Na42 3.58(1)		In20 2.932(4)		Na55 3.42(2)		Na51 3.53(1)	In22	3.006(3)
	In18 3.074(3)		Na46 3.37(1)		In40 3.121(3)		Na64 3.47(1)		Na56 3.43(1)	Na17	3.36(1)
	In23 2.994(3)		Na48 3.37(1)		Na15 3.50(2)		Na67 3.29(2)		Na61 3.35(1)	Na22	3.39(1)
	Na9 3.54(1)		Na55 3.41(1)		Na23 3.30(1)		<b>In19</b>		Na64 3.42(1)	Na24	3.38(1)
	Na24 3.41(1)		Na58 3.50(1)		Na30 3.235(2)		In13 3.116(4)		Na66 3.46(2)	Na28	3.38(1)
	Na26 3.41(1)		<b>In9</b>		Na39 3.69(2)	2	In40 2.938(3)		<b>In24</b>	Na42	3.54(1)
	Na27 3.36(8)		In9 3.018(4)		Na52 3.47(1)	2	In53 2.75(2)		In25 2.990(3)	Na56	3.43(1)
	Na35 3.31(1)		In27 2.974(3)		Na65 3.52(1)		InC1 2.887(6)		In27 3.070(4)	Na58	3.51(1)
	Na56 3.43(1)		In34 3.041(4)		<b>In14</b>		Na15 3.55(2)		In29 2.916(3)	Na63	3.49(1)
	Na64 3.49(1)		In47 2.986(4)		In4 2.955(5)		Na37 3.58(2)		In41 3.032(3)		<b>In29</b>
	Na68 3.48(1)		Na3 3.52(1)		2 In20 2.935(3)		Na60 3.37(1)		Na3 3.523(9)	In16	3.064(3)
	<b>In4</b>		Na14 3.41(1)		2 In43 3.144(4)		2 Na65 3.53(1)		Na7 3.45(1)	In24	2.916(3)
	In4 3.030(7)		Na16 3.42(1)		Na4 3.49(2)		<b>In20</b>		Na10 3.344(8)	In31	3.019(3)
	In14 2.955(5)		Na19 3.37(2)		Na39 3.56(2)		In13 2.932(4)		Na11 3.53(1)	In39	2.993(3)
2	In42 3.020(4)		Na41 3.40(1)		2 Na49 3.49(1)		In14 2.935(3)		Na33 3.54(1)	In52	3.408(6)
	Na4 3.50(2)		Na54 3.33(1)		2 Na57 3.34(1)		In39 2.925(3)		Na40 3.38(1)	Na2	3.26(1)
	Na8 3.62(2)		Na59 3.55(2)		<b>In15</b>		In40 3.159(3)		Na52 3.39(1)	Na7	3.47(1)
2	Na47 3.30(2)		Na62 3.35(1)		In7 3.121(4)		In43 3.112(3)		Na62 3.37(1)	Na11	3.59(1)
2	Na49 3.55(1)		<b>In10</b>		In13 2.954(4)		Na11 3.54(1)		<b>In25</b>	Na33	3.48(1)
2	Na57 3.46(2)		In6 3.044(3)		In15 3.089(5)		Na23 3.29(1)		In24 2.990(3)	Na36	3.59(1)
	<b>In5</b>		In21 2.979(3)		In36 2.977(3)		Na39 3.574(6)		In25 3.028(5)	Na40	3.29(1)
	In17 2.961(4)		In30 3.000(3)		In46 3.046(4)		Na49 3.56(1)		In42 2.980(4)	Na47	3.47(1)
2	In37 3.052(4)		In47 3.025(3)		Na15 3.41(1)		Na52 3.48(1)		In50 3.040(4)	Na57	3.39(1)
	In46 3.061(6)		Na14 3.25(1)		Na23 3.62(1)		Na57 3.39(1)		Na3 3.55(2)		<b>In21</b>
	Na9 3.60(2)		Na20 3.42(1)		Na30 3.507(2)		<b>In21</b>		Na7 3.35(1)		In10 2.979(3)
	Na34 3.40(2)		Na21 3.466(8)		Na34 3.60(2)		In10 2.979(3)		Na8 3.524(7)		In14 2.935(3)
2	Na38 3.44(2)		Na22 3.32(1)		Na44 3.46(1)		In21 3.043(5)		Na10 3.43(2)		In39 2.925(3)
2	Na44 3.41(1)		Na29 3.38(1)		Na52 3.66(1)		In32 2.999(3)		Na40 3.30(1)		In40 3.159(3)
2	Na68 3.44(1)		Na42 3.56(1)		Na65 3.37(1)		In35 3.077(4)		Na52 3.39(1)		In43 3.112(3)
	<b>In6</b>		Na53 3.27(1)		<b>In16</b>		Na5 3.42(1)		Na57 3.37(1)		<b>In21</b>
	In6 3.043(4)		Na59 3.548(9)		In7 3.091(5)		Na6 3.37(1)		<b>In25</b>		In10 2.979(3)
	In10 3.044(3)		<b>In11</b>		2 In29 3.064(3)		Na20 3.40(1)		In24 2.990(3)		In14 2.935(3)
	In28 2.967(4)		In32 3.036(5)		2 In39 3.107(4)		Na22 3.32(1)		In42 2.980(4)		In39 2.925(3)
	In47 2.975(4)		2 In37 3.097(4)		Na2 3.57(2)		Na29 3.40(1)		In50 3.040(4)		In52 3.392(5)
	Na17 3.34(2)	2	In44 3.044(3)		Na23 3.30(2)		Na42 3.64(1)		Na3 3.55(2)		2 Na14 3.29(1)
	Na19 3.34(2)	2	Na18 3.62(2)		2 Na33 3.27(1)		Na43 3.57(2)		Na7 3.35(1)		2 Na21 3.38(1)
	Na21 3.42(2)		2 Na20 3.26(1)		Na36 3.53(2)		Na53 3.29(2)		Na8 3.524(7)		2 Na29 3.41(2)
	Na22 3.39(1)		Na31 3.62(2)		2 Na52 3.60(1)				Na10 3.43(2)		Na53 3.22(2)
	Na28 3.32(2)		Na34 3.59(2)						Na40 3.30(1)		2 Na59 3.50(2)
	Na42 3.56(1)	2	Na42 3.50(1)						Na47 3.42(1)		<b>In31</b>
	Na59 3.49(2)								Na50 3.378(8)		In29 3.019(3)
	Na63 3.55(2)								Na62 3.41(1)		In38 2.989(4)
									<b>In26</b>		In42 2.925(3)
									In33 2.982(5)		In45 3.056(3)
									2 In39 3.067(4)		In52 3.392(5)
									2 In52 3.337(5)		Na2 3.27(1)
									Na2 3.41(2)		Na4 3.605(9)
									2 Na7 3.58(1)		Na7 3.48(1)
									Na47 3.12(2)		Na13 3.482(9)
									2 Na49 3.67(1)		Na36 3.60(1)
									Na57 3.27(2)		Na40 3.30(1)
											Na49 3.55(1)

TABLE 3—Continued

<b>In32</b>		<b>In37</b>		<b>In41</b>		<b>In45</b>		<b>In50</b>		<b>InA1</b>	
	In11 3.036(5)	In5 3.052(4)	In24 3.032(3)	2	In31 3.056(3)	2	In25 3.040(4)		NiA 2.711(6)		
2	In21 3.000(3)	In11 3.097(4)	In27 3.024(4)	2	In38 3.108(4)		In34 2.925(5)		InA1 0.97(1)		
2	In35 3.119(4)	In12 3.024(4)	In40 2.959(3)		In45 3.050(7)		In50 2.948(7)		InA2 3.70(1)		
	Na5 3.56(1)	In37 3.078(5)	In41 3.049(5)		Na2 3.59(2)		Na3 3.53(2)		InA2 3.13(1)		
	Na6 3.76(1)	In44 3.049(4)	Na3 3.56(2)	2	Na4 3.57(2)		Na8 3.44(2)		InA3 2.10(1)		
	Na18 3.54(2)	Na9 3.49(2)	Na10 3.33(1)	2	Na13 3.30(2)		2	Na45 3.37(2)	InA3 2.97(1)		
2	Na20 3.30(1)	Na18 3.63(2)	Na11 3.53(1)		Na32 3.30(2)		2	Na50 3.39(1)	InA4 3.02(1)		
2	Na42 3.51(1)	Na34 3.68(1)	Na16 3.28(1)		Na36 3.51(2)		2	Na62 3.40(1)	InA4 3.67(1)		
	<b>In33</b>	Na42 3.49(1)	Na25 3.43(2)		<b>In46</b>		<b>In51</b>		InA5 3.074(8)		
	In26 2.982(5)	Na44 3.46(1)	Na52 3.42(1)		In5 3.061(6)		In22 3.119(6)		InA5 3.334(9)		
2	In38 3.066(4)	Na63 3.29(1)	Na60 3.50(2)	2	In15 3.046(4)		2	In48 3.083(4)	InA6 3.208(9)		
2	In52 3.340(5)	Na68 3.30(1)	Na65 3.54(1)		In46 2.943(7)		In49 3.184(5)		InA6 3.338(9)		
	Na2 3.44(2)	<b>In38</b>	<b>In42</b>	2	Na15 3.62(2)		2	Na24 3.55(1)	Na31 3.56(2)		
2	Na7 3.59(1)	In31 2.989(4)	In4 3.020(4)		Na30 3.60(5)		2	Na48 3.38(1)	Na33 3.05(1)		
	Na10 3.11(2)	In33 3.066(4)	In25 2.980(4)		Na34 3.36(2)		2	Na58 3.40(1)	Na33 3.62(1)		
2	Na11 3.65(1)	In38 3.037(5)	In31 2.925(3)	2	Na38 3.42(2)		2	Na67 3.26(2)	Na36 3.50(2)		
	Na25 3.25(2)	In43 2.933(4)	In42 3.079(5)	2	Na44 3.42(1)				Na40 3.91(1)		
	<b>In34</b>	In45 3.108(4)	Na4 3.46(1)		<b>In47</b>		<b>In52</b>		Na54 3.93(1)		
	In1 2.932(4)	In52 3.377(5)	Na7 3.45(1)		In6 2.975(4)		In26 3.337(5)		NiA 2.74(1)		
2	In9 3.041(4)	Na2 3.60(1)	Na8 3.547(8)		In9 2.986(4)		In29 3.408(6)		2	InA1 3.70(1)	
	In50 2.925(5)	Na4 3.582(9)	Na13 3.55(2)		In10 3.025(3)		In31 3.392(5)		2	InA1 3.13(1)	
	Na3 3.49(2)	Na11 3.53(1)	Na40 3.39(1)		In44 2.919(3)		In33 3.340(5)		2	InA3 2.30(1)	
2	Na14 3.40(1)	Na25 3.49(2)	Na47 3.325(9)		Na14 3.36(1)		In38 3.377(5)		2	InA4 3.18(1)	
2	Na45 3.43(1)	Na32 3.553(6)	Na49 3.50(1)		Na19 3.37(1)		In39 3.380(5)		2	InA5 2.95(2)	
	Na59 3.50(2)	Na49 3.38(1)	Na50 3.33(1)		Na20 3.53(1)		In52 3.104(8)			InA5 1.33(2)	
2	Na62 3.35(1)	<b>In39</b>	<b>In43</b>		Na41 3.44(1)		Na2 3.14(1)				
	<b>In35</b>	In16 3.107(4)	In14 3.144(4)		Na42 3.55(1)		Na7 3.48(1)			Na13 3.38(2)	
	In8 3.077(3)	In20 2.925(3)	In20 3.112(3)		Na54 3.33(1)		Na7 3.51(1)		2	Na40 3.38(1)	
	In21 3.077(4)	In26 3.067(4)	In38 2.933(4)		Na59 3.56(1)		Na49 3.95(1)			Na50 3.54(2)	
	In32 3.119(4)	In29 2.993(3)	In40 2.932(4)		Na63 3.50(2)		<b>In53</b>				
	In35 3.022(5)	In39 3.036(5)	In43 2.950(5)		<b>In48</b>		In19 2.75(2)			NiA 2.801(8)	
	Na6 3.521(5)	In52 3.380(5)	In53 2.82(2)		In23 3.146(4)		2	In40 2.83(1)		InA1 2.10(1)	
	Na12 3.38(2)	Na2 3.56(2)	Na4 3.45(1)		In48 3.126(5)		2	In43 2.82(2)		InA1 2.97(1)	
	Na18 3.66(2)	Na11 3.40(1)	Na11 3.51(1)		In49 3.181(4)			In53 2.72(4)		InA2 2.30(1)	
	Na22 3.26(1)	Na23 3.57(1)	Na25 3.44(1)		In51 3.083(4)		2	Na25 3.83(2)		InA2 3.02(1)	
	Na42 3.67(1)	Na49 3.55(1)	Na32 3.34(1)		Na12 3.41(2)			Na32 3.69(3)		InA3 3.22(2)	
	Na43 3.58(1)	Na52 3.63(1)	Na37 3.65(1)		Na24 3.49(1)			Na37 1.36(2)		InA4 1.46(1)	
	Na46 3.31(1)	Na57 3.47(2)	Na49 3.53(1)		Na46 3.31(1)		2	Na60 3.68(2)		InA4 3.02(1)	
	Na55 3.40(2)	<b>In40</b>	<b>In44</b>		Na48 3.36(1)					InA5 3.14(1)	
	<b>In36</b>	In13 3.121(3)	In11 3.044(3)		Na61 3.554(8)		<b>NiA</b>			InA6 3.06(1)	
	In7 3.033(3)	In19 2.938(3)	In36 3.043(4)		Na64 3.39(1)		4	InA1 2.711(6)		InA6 3.66(1)	
	In15 2.977(3)	In20 3.159(3)	In37 3.049(4)		Na66 3.33(1)		2	InA2 2.74(1)		Na33 3.74(2)	
	In27 2.943(3)	In41 2.959(3)	In47 2.919(3)		<b>In49</b>		2	InA3 2.801(8)		Na40 3.63(2)	
	In44 3.043(4)	In43 2.932(4)	Na20 3.44(1)		In22 2.971(5)		4	InA4 2.750(7)		Na45 3.76(2)	
	Na31 3.57(2)	In53 2.83(1)	Na31 3.61(1)		2	In23 2.980(3)	4	InA5 2.68(1)		Na54 3.27(2)	
	Na33 3.44(1)	Na11 3.46(1)	Na34 3.25(1)	2	2	In48 3.181(4)	2	InA6 2.700(8)		Na62 3.40(1)	
	Na34 3.28(1)	Na25 3.35(1)	Na41 3.43(1)			In51 3.184(5)					
	Na41 3.38(1)	Na37 3.655(6)	Na42 3.57(1)		2	Na24 3.53(1)					
	Na44 3.44(1)	Na52 3.46(1)	Na44 3.38(1)		2	Na51 3.41(1)					
	Na52 3.63(1)	Na60 3.31(1)	Na54 3.30(1)		2	Na56 3.37(1)					
	Na54 3.23(1)	Na65 3.45(1)	Na63 3.46(1)			Na61 3.45(1)					
	Na65 3.60(1)										

(continued)



TABLE 3—Continued

Na13		Na18		Na23		Na28		Na34		Na39		
2	In31 3.482(9)	2	In8 3.60(1)		In7 3.35(2)	2	In6 3.32(1)		In5 3.39(2)	4	In13 3.69(2)	
2	In42 3.55(2)		In11 3.62(2)	2	In13 3.30(1)		In22 3.26(2)		In7 3.61(2)	2	In14 3.56(2)	
2	In45 3.30(2)	2	In12 3.56(1)	2	In15 3.62(1)	2	In28 3.38(1)		In11 3.59(2)	4	In20 3.574(6)	
	InA2 3.38(2)	2	In18 3.57(2)		In16 3.30(2)	2	InB1 3.36(2)	2	In15 3.60(2)	2	Na23 3.40(2)	
	InA5 2.92(2)		In32 3.54(2)	2	In20 3.29(1)		Na21 3.25(2)	2	In36 3.28(1)		Na30 3.33(3)	
	InA5 3.93(2)	2	In35 3.66(2)	2	In39 3.57(1)	2	Na22 3.49(1)	2	In37 3.68(1)	2	Na57 3.45(3)	
	Na4 3.53(2)	2	In37 3.63(2)		Na30 3.86(2)	2	Na58 3.33(2)	2	In44 3.25(1)			
	Na13 3.98(4)		Na9 3.65(3)		Na39 3.40(2)		Na29		In46 3.36(2)		Na40	
2	Na36 3.81(2)	2	Na42 3.60(2)	2	Na52 3.52(1)	2	In10 3.38(1)		Na31 3.40(3)		In24 3.38(1)	
2	Na40 3.35(2)		Na55 3.48(3)		Na24	2	In21 3.40(1)	2	Na44 3.21(2)		In25 3.30(1)	
	Na50 3.76(2)		Na19		In3 3.41(1)	2	In30 3.41(2)		Na35		In29 3.29(1)	
	Na14	2	In6 3.34(2)		In8 3.50(1)	2	InA4 3.47(2)		In2 3.32(2)		In31 3.30(1)	
	In1 3.40(1)	2	In9 3.37(2)		In12 3.71(1)	2	InA6 3.72(2)	2	In3 3.31(1)		In42 3.39(1)	
	In9 3.41(1)	2	In47 3.37(1)		In18 3.49(1)		Na5 3.33(2)	2	In23 3.28(2)		InA1 3.91(1)	
	In10 3.25(1)		InC4 3.28(2)		In22 3.42(1)	2	Na14 3.29(2)	2	InB2 3.18(2)		InA2 3.38(1)	
	In30 3.29(1)		Na17 3.31(3)		In23 3.36(1)	2	Na20 3.38(1)	2	InB4 3.66(2)		InA3 3.63(2)	
	In34 3.40(1)	2	Na41 3.40(2)		In28 3.38(1)		Na30	2	InB5 3.62(2)		InA5 3.70(1)	
	In47 3.36(1)		Na59 3.39(3)		In48 3.49(1)	4	In13 3.235(2)	2	Na27 3.35(2)		Na13 3.35(2)	
	InA4 3.41(1)	2	Na63 3.39(2)		In49 3.53(1)	4	In15 3.507(2)	2	Na64 3.34(2)		Na33 3.41(2)	
	Na14 3.86(3)		Na20		In51 3.55(1)	2	In46 3.601(5)	2	Na66 3.52(3)		Na36 3.36(1)	
	Na20 3.89(2)		In10 3.42(1)		Na48 3.86(2)	2	Na15 3.62(2)		Na36		Na50 3.29(2)	
	Na29 3.29(2)		In11 3.26(1)		Na56 3.46(2)	2	Na23 3.86(2)		In16 3.53(2)		Na62 3.29(2)	
	Na45 3.36(2)		In21 3.40(1)		Na58 3.36(2)		Na39 3.33(3)		Na37		Na41	
	Na54 3.34(2)		In32 3.30(1)		Na64 3.28(2)		Na31	2	In29 3.59(1)		In9 3.40(1)	
	Na59 3.37(2)		In44 3.44(1)		Na25		In7 3.47(2)	2	In31 3.60(1)		In27 3.43(1)	
	Na62 3.83(2)		In47 3.53(1)		In33 3.25(2)		In11 3.62(2)	2	In45 3.51(2)		In36 3.38(1)	
	Na15		InA4 3.84(1)		2	In38 3.49(2)	2	In36 3.57(2)	2	InA1 3.50(2)		In44 3.43(1)
2	In13 3.50(2)		InA6 3.08(1)		2	In40 3.35(1)	2	In44 3.61(1)	2	InA5 3.65(2)		In47 3.44(1)
2	In15 3.41(1)		InA6 3.59(1)		2	In41 3.43(2)	2	InA1 3.56(2)	2	Na2 3.36(2)		InC2 3.66(1)
	In19 3.55(2)		Na5 3.86(2)		2	In43 3.44(1)	2	InA6 3.61(2)	2	Na13 3.81(2)		InC3 3.47(2)
2	In46 3.62(2)		Na14 3.89(2)		2	In53 3.83(2)	2	Na20 3.82(2)	2	Na33 3.86(2)		InC4 3.70(1)
	InC1 3.45(2)		Na20 3.85(3)			Na10 3.61(3)	2	Na33 3.79(2)	2	Na40 3.36(1)		Na16 3.47(2)
2	InC3 3.59(2)		Na29 3.38(1)			Na11 3.47(1)	2	Na34 3.40(3)		Na37		Na19 3.40(2)
	Na30 3.62(2)		Na31 3.82(2)			Na37 3.58(2)	2	Na54 3.31(1)	2	In19 3.58(2)		Na44 3.33(2)
	Na38 3.44(3)		Na42 3.49(2)			Na60 3.99(2)		Na32	4	In40 3.655(6)		Na63 3.40(2)
2	Na65 3.74(2)		Na54 3.42(2)			Na26	4	In38 3.553(6)	4	In43 3.65(1)		Na65 3.38(2)
	Na16	2	In6 3.42(2)			In2 3.37(2)	4	In43 3.34(1)	2	In53 1.36(2)		Na42
	In9 3.42(1)	2	In10 3.466(8)			2	In3 3.41(1)	2	In45 3.30(2)		In6 3.56(1)	
2	In27 3.328(7)	2	In30 3.38(1)			2	In23 3.39(1)	2	In53 3.69(3)	2	In8 3.58(1)	
2	In41 3.28(1)		InB1 3.78(2)			2	InC5 3.96(2)	2	Na4 3.43(2)	2	In10 3.56(1)	
	InC2 3.12(2)	2	Na21 3.78(3)			2	InC6 3.16(2)	2	Na37 3.44(4)	2	In11 3.50(1)	
	Na3 3.31(2)		Na22 3.93(1)				Na51 3.35(2)		Na33	2	In12 3.46(1)	
2	Na41 3.47(2)		Na28 3.25(2)				2	Na56 3.38(1)	2	In5 3.45(1)		
	Na60 3.73(3)	2	Na53 3.36(2)				2	Na68 3.40(2)		In17 3.49(2)		
2	Na65 3.85(2)		Na59 3.36(2)					Na27	2	In46 3.42(2)		
	Na17		Na22					In2 3.47(1)	2	InC3 3.61(2)		
	In6 3.34(2)		In6 3.39(1)					2	In3 3.362(8)	2	InC6 3.33(2)	
	In22 3.35(2)		In8 3.32(1)					2	In18 3.37(2)		Na15 3.44(3)	
2	In28 3.36(1)		In10 3.32(1)					2	InB2 3.26(2)	2	Na44 3.39(1)	
	InC4 3.18(2)		In21 3.32(1)						Na9 3.44(2)	2	Na68 3.43(2)	
	InC5 3.83(2)		In28 3.39(1)						Na27 3.99(3)		Na18 3.60(2)	
2	InC7 3.83(2)		In35 3.26(1)						2	Na35 3.35(2)		
	Na19 3.31(3)		InB1 3.04(1)						2	Na64 3.81(2)		
2	Na56 3.39(2)		Na21 3.93(1)						Na31 3.79(2)		Na20 3.49(2)	
2	Na63 3.41(1)		Na28 3.49(1)						Na33 3.95(2)		Na22 3.31(2)	
			Na42 3.31(2)						Na36 3.86(2)		Na63 3.56(2)	
			Na43 3.79(2)						Na40 3.41(2)			
			Na46 3.61(2)						Na52 3.44(2)			
			Na53 3.42(1)						Na54 3.32(2)			
			Na58 3.92(2)						Na62 3.83(2)			

(continued)



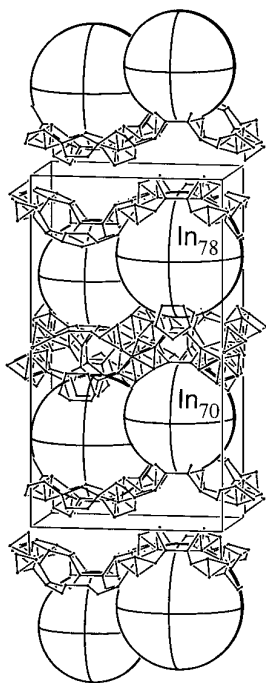


FIG. 1. A general view of the unit cell of  $\text{Na}_{-172}\text{In}_{-197}\text{Ni}_2$  approximately along the  $a$  axis ( $c$  is vertical). The  $\text{In}_{70}$  and  $\text{In}_{78}$  fulleranes are shown only as large spheres. All In-In bonds to atoms between the spheres that are less than 4.00 Å apart are drawn.

significant atomic rearrangements.) We should point out that  $D_{3h}$ -I is the only nearly spherical isomer; the rest are quite oblong in shape.

The two pentagons in the waist of  $\text{In}_{78}$  (Fig. 3) generated by In5, 17, and 46 (and mirror planes) are shared with

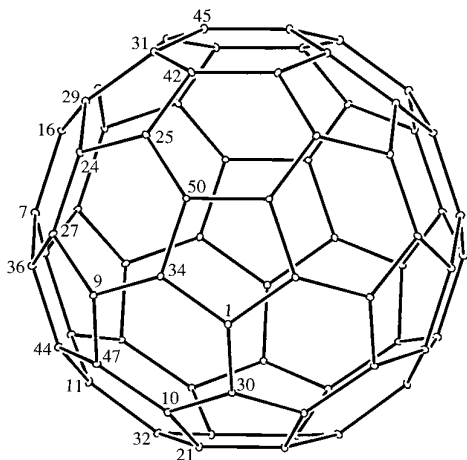


FIG. 2. A nearly [100] view of the  $\text{In}_{70}$  fullerane (A) with  $C_{2v}$  symmetry (the 2-fold axis is vertical). It has a pseudo  $D_{3h}$  symmetry (as does  $C_{70}$ ) with the pseudo 5-fold axis approximately along the view direction (30% probability displacement ellipsoids).

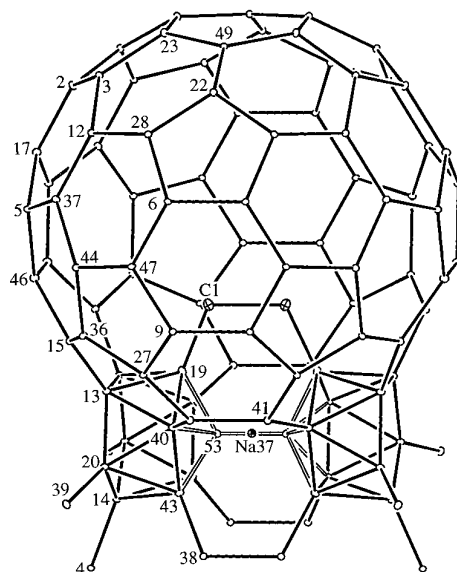


FIG. 3. A nearly [010] view of the  $\text{In}_{78}$  fullerane (C) with  $C_{2v}$  symmetry. (The 2-fold axis is vertical and the mirror planes lie approximately in and normal to the page.) The cage has pseudo  $D_{3h}$  symmetry with the 3-fold axis approximately along the view direction (through the hexagons made of In6, 9, 47 plus the mirror images). The two lower pentagons are parts of two *nido*- $\text{In}_{11}$  (shown left and right), the exo bonds from which provide connectivity to  $\text{In}_{70}$  cages. The inner In19 provides connection to InC1 (labeled as C1) which is part of encapsulated 2-bonded  $\text{In}_{16}$  inner cluster (not shown). The two In53 and the intervening Na37 (open bonds) refine with occupancies of 30(2) and 85(5)%, respectively (30% ellipsoids).

those in two other  $\text{In}_{78}$  cages in a string along the  $a$  axis. The four pentagons In9, 27, 36, 44, 47 that lie below the waist in this view, two in front and two in back, are shared with four  $\text{In}_{70}$  cages. As can be seen, the two pentagons defined by In13, 40, and 53 are parts of two *nido*-icosahedra in which In19 caps each pentagon from inside the cage and is bonded to InC1, part of an encapsulated cluster at the center of the cage. (Neither In19 or InC1 is included in the  $\text{In}_{78}$  count.) The more general relationships of this arrangement to other centered cage structures as well as to  $\beta$ -B will appear later along with a picture of the whole unit.

The remaining atoms of the foregoing icosahedra lie outside the cage and are all exo bonded. In53 is the atom that refined to 30(2)% occupancy (17(1)% for the second crystal) and lies 1.4 Å from Na37 (Fig. 3), which refined with 85(5)% occupancy (84(7)% for the second crystal). The fact that the In53 and Na37 sites are so close means that when one is occupied, the other must be empty. This combined with the fact that the sum of the occupancies of the two positions, 115(5)% (101(7)% for the second crystal), falls within  $3\sigma$  of 100% suggest that only *arachno*- $\text{In}_{76}$  (75–80%) and *closo*- $\text{In}_{78}$  (25–20%) species actually exist throughout the structure. (The presence of any *nido*- $\text{In}_{77}$  would lead to lower occupancy of the In53 site.) For purposes of clarity, the cage will still be referred to as  $\text{In}_{78}$

throughout the text. The distance between the two In53 atoms (2.72(4) Å) and between each In53 and the nearest In19, In43, In40 in the icosahedra (2.75(2) Å, 2.82(2) Å, and 2.83(1), respectively) are a little short compared with the usual 2.85 Å and above that are observed between atoms with delocalized bonding. A similar situation within a row of *arachno*-icosahedra with very close vertices was encountered in Na<sub>15</sub>In<sub>27.4</sub> (12). In that case, a pair of indium atoms that each refined with 54.1(9)% occupancy cap a pair of *arachno*-polyhedra. These are also very close to the polyhedral atoms (2.788(6), 2.889(3), and 2.841(5) Å) and to each other (2.76(1) Å). It was not clear in that structure, though, whether some of the icosahedra are bonded via such atoms, or simply alternating *closo* and *arachno* species are present.

A comparison of the distances distributions in In<sub>78</sub>, especially the shorter In53–In53 member, with those in the D<sub>3h</sub>-I isomer of C<sub>78</sub> results in a surprising similarity. Distances between all carbon atoms of the five possible isomers for C<sub>78</sub> calculated by an *ab initio* method (18) also show the corresponding separation in the D<sub>3h</sub>-I isomer to be shorter than the rest, 1.338 vs 1.381–1.493 Å.

#### Layer Interconnections

A magnified section of the unit cell near  $z = 1/2$  in Fig. 4a shows the connectivities between the two In<sub>70</sub>, In<sub>78</sub> layers that generate the double layers of fused fullerenes, while the central pair of cages have been separated and enlarged in Fig. 4b so that the atoms forming the attachments can be seen more easily and also labeled. The In<sub>78</sub> portions are practically the same as in Fig. 3 except that cage is now represented as a sphere, and the view has been rotated about 90° around the vertical *c* axis. (The thermal ellipsoid axial markings are accidentally coincident with the two proper mirror planes.) As mentioned earlier, the hexagons of In16, 29, 31, and 45 in In<sub>70</sub>, Fig. 2, are also parts of *nido*-In<sub>14</sub> “warts” on the surface, as shown in Fig. 4b. (The corresponding *closo*-deltahedron is the 15-vertex tricapped truncated trigonal prism. The two triangular basal faces of the prism are (In45, 38, 38) on one end and (In16, 39, 39) on the other, while the triangles formed from the truncated corners are (In33, 38, 38), two (In31, 45, 38), (26, 39, 39), and two (In16, 29, 39). We have seen the same type of cluster, i.e., a 15-vertex tricapped truncated trigonal prism, in Na<sub>23</sub>In<sub>38</sub>Zn<sub>4.6</sub> and in Na<sub>23</sub>In<sub>39</sub>Au<sub>3.4</sub> (11).) The derivative in this case is *nido* with the atom that would cap the hexagonal face In16, 29, 31, 45 from inside the cage being a sodium atom instead (below). The six-bonded capping atoms are two partially occupied In52 (Fig. 4b). This deltahedron is 12-bonded. Six bonds are from In16, 29, 31, and 45 to other atoms of the fullerene. The two In39 atoms connect the In<sub>70</sub> cage to two In<sub>78</sub> cages in the same layer through exo bonds to In20 of the attached

*nido*-icosahedra (Figs. 4a, 4b). Finally, the two In38 atoms connect the In<sub>70</sub> group to two In<sub>78</sub> cages in the next layer via In43 in the *nido*-icosahedra. The two In26, 33 atoms of the *nido*-In<sub>14</sub> on the In<sub>70</sub> fullerene lack exo bonds, and lone pairs of electrons are presumably associated with them.

The capping atoms In52 are exo bonded to the same type of atom in clusters attached to In<sub>70</sub> in the next layer. The In52 atoms refine with not much more than half occupancy (59(1)%) which suggests that when one position is occupied, the symmetry-related one in the neighboring cluster is probably empty so that the seventh In52–In52 bond does not exist, as discussed earlier. On the other hand, such atoms in a 12-bonded *closo*-In<sub>16</sub> cluster in Na<sub>15</sub>In<sub>27.4</sub> were refined with full occupancy, although they are exo bonded to their equivalents in the next cluster (12). Nevertheless, it seems that seven like neighbors for indium are quite unfavorable. One more connection between the two layers within a double layer is achieved via an exo bond from In14 of the *nido*-icosahedra to In4. The latter is also bonded to two In42 atoms in the In<sub>70</sub> cage and to another In4 which, in turn, is bonded to the next In<sub>70</sub> cage.

In summary, the bonding pattern *inside* the double layer (Fig. 4) discussed above is as follows: (a) Each In<sub>70</sub> is connected to two other In<sub>70</sub> cages within one layer by sharing two pentagonal faces and also through the In4–In4 pair of exo atoms (all along *a*). The last are very much like the In10–In10 exobonds between In<sub>74</sub> seen earlier (5). There are also intercage bonds In9–In9, In30–In30, and In25–In25. (b) The same framework is connected to four In<sub>78</sub> cages within one layer by sharing four pentagonal faces and also through the In39–In20 pair of exo atoms; (c) The same (In<sub>70</sub>) cage is connected to one In<sub>78</sub> cage from the next layer of a bilayer through the two In38–In43 and In4–In14 pairs of exo atoms; (d) The same In<sub>70</sub> would have been connected to four other In<sub>70</sub> cages from the next layer had the In52 site been fully occupied, not 59(1)%; (e) Each In<sub>78</sub> is connected to two other In<sub>78</sub> cages within the same layer (row) via two shared pentagonal faces, plus four parallel bonds from nearest-neighbor atoms, as in (a); (f) the same In<sub>78</sub> is connected to one In<sub>70</sub> in the next layer via six pairs of exo atoms, two In14–In4 and four In43–In38. We will return to the endohedral components of these two cages later.

Next, we turn our attention to the bonding pattern *outside* the double layers. Figure 5 shows a magnified section of the unit cell near  $z = 0$  where parts of two neighboring bilayers can be seen. The space between them is filled with sodium cations and also with NiB-centered M<sub>60</sub> cages (below). If exo indium atoms were not present on this side of the double layer, many atoms on the surfaces would be only three-bonded. Unlike carbon in the fullerenes, where each atom has three  $\sigma$ -bonds but is also  $\pi$ -bonded, the

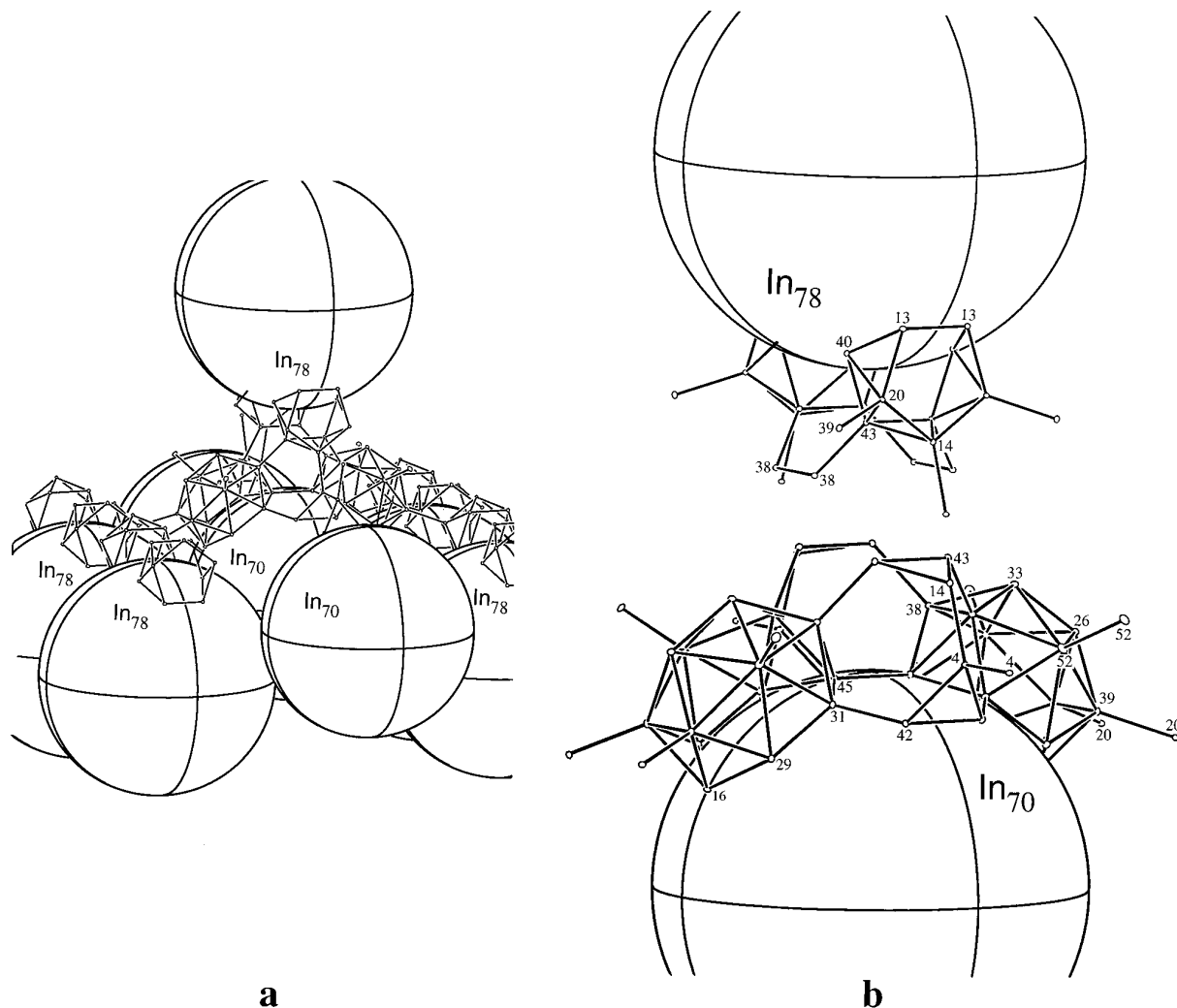


**FIG. 4.** (a) An enlarged section of the unit cell of  $\text{Na}_{172}\text{In}_{197}\text{Ni}_2$  near  $z = 1/2$  (see Fig. 1) where two layers of mixed fulleranes are interconnected to form a double layer via exo indium atoms. (b) The  $\text{In}_{78}$  and  $\text{In}_{70}$  components separated to show the *nido*- $\text{In}_{11}$  and *nido*- $\text{In}_{14}$ , respectively, attached to them. The two mirror planes drawn through the  $\text{In}_{70}$  spheres contain  $\text{In}_4$ , 14, and  $\text{In}_{26}$ , 33, respectively.

indium atoms generally require at least four  $\sigma$ -bonds. A three-bonded state appears to be very unlikely for indium, although a rare precedent has been found in the structure of  $\text{K}_{15}\text{Na}_8\text{In}_{39}$  (two nonplanar three-bonded indium atoms form a rectangle by alternating with two four-bonded ones (11)). This is the only case, so far, where formally  $sp^2$  hybridized (or better, intermediate  $sp^2$ - $sp^3$ ) indium atoms appear to be involved in relatively well pronounced  $\pi$ -bonding. An example for thallium is found in  $\text{Tl}_3^{7-}$  (20).

Figure 5 shows how a number of hexagons and triangles (outlined with open bonds) are instead generated by exo atoms to avert this problem. (As a matter of fact, the exo atoms between the two layers forming the bilayers play the same role for the atoms on the inward-facing surface of these cages.) Each such triangle ( $\text{In}_{48}$ , 51) is bonded near the pole of an  $\text{In}_{78}$  cage (to  $\text{In}_{49}$ , 22, 23 ( $\times 2$ )), while

each hexagon ( $\text{In}_8$ , 18, 35) is bonded to two  $\text{In}_{78}$  cages ( $\text{In}_3$ , 12, 28) and one  $\text{In}_{70}$  cage ( $\text{In}_{21}$ , 32). (The bonds within the hexagons also connect  $\text{In}_{78}$  to  $\text{In}_{78}$  and  $\text{In}_{70}$  to  $\text{In}_{78}$  via exo-bonds, just as for the  $\text{In}_4$ - $\text{In}_4$  noted two paragraphs above. Notice that each triangle has an opposed and substantially parallel hexagon in the other layer, and vice versa. The closest approach between the two layers occurs between the atoms in these “decorations,” but these remain very long, 5.41 Å for  $\text{In}_{35}$ - $\text{In}_{48}$ , 5.46 Å for  $\text{In}_8$ - $\text{In}_{48}$ , and 5.46 Å for  $\text{In}_{18}$ - $\text{In}_{51}$ . The picture is very reminiscent of the hexagon and triangle augmentation found on the surface of and between the individual layers of condensed  $\text{In}_{74}$  in  $\text{Na}_{96}\text{In}_{97}\text{Z}_2$  (5). It can be seen in Fig. 5 that four  $\text{In}_{78}$  and two  $\text{In}_{70}$  cages, four hexagons, and four triangles surround a cavity with nearly spherical coordination. These together with some Na atoms define the  $M_{60}$  fullerane, and



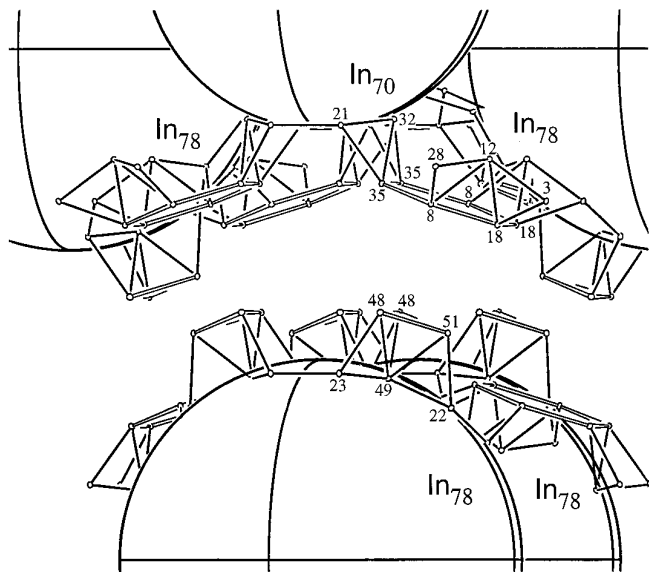


FIG. 5. An enlarged section of the unit cell of  $\text{Na}_{172}\text{In}_{197}\text{Ni}_2$  near  $z = 0$  where four spheres from one layer (one  $\text{In}_{70}$  in the top back cannot be seen) approach two spheres from another layer at the bottom section. Bonds within the hexagonal and triangular formations of exo indium atoms are drawn as open lines.

at its center we find the second isolated Ni-centered indium cluster  $B$ .

$M_{60}$

At this point, the second way of describing the structure is needed in order to ease its further comprehension. It

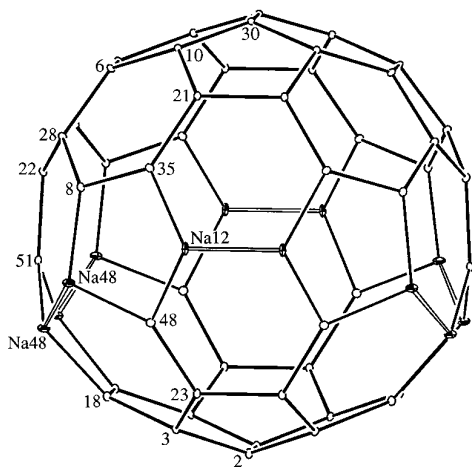
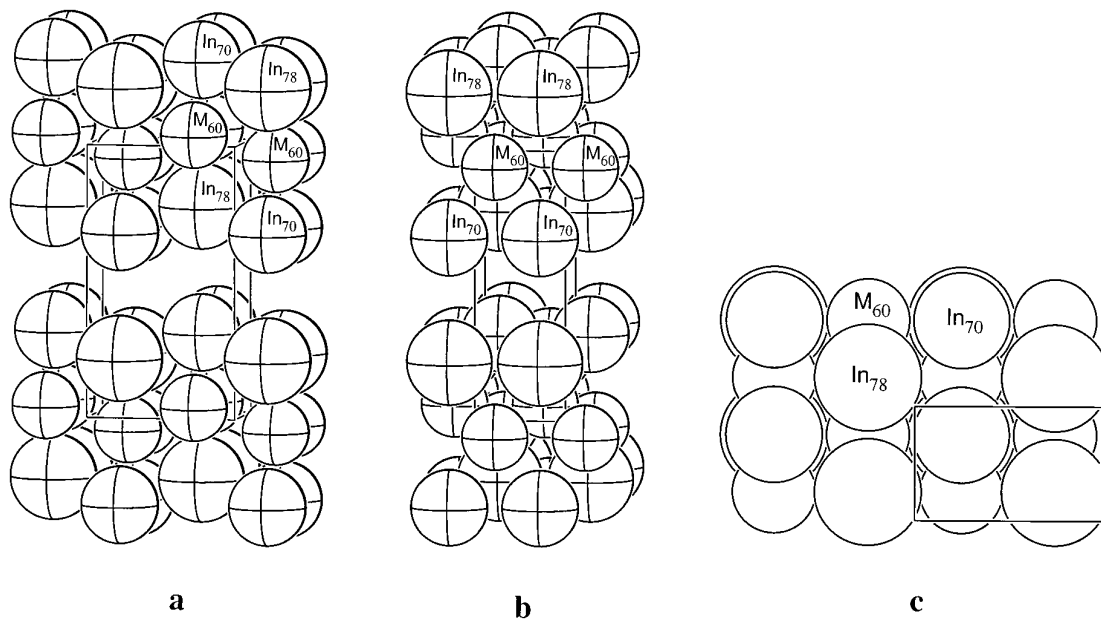


FIG. 6. A nearly  $[100]$  view of the  $M_{60}$  fullerane of 48 indium and 12 sodium (shaded) atoms ( $C_{2v}$  symmetry). The six edges defined by pairs of Na12 or Na48 near the waist (open interconnections) are shared with six other  $M_{60}$  cages. The six pentagons that do not contain sodium atoms are all shared with fullerenes, four  $\text{In}_{78}$  and two  $\text{In}_{70}$ . The two-fold axis ( $c$  axis) is vertical (30% thermal ellipsoids).

was mentioned before that sodium cations fill the space between the bilayers. Two among them, Na12 and 48, have special positioning such that another type of a fullerane cage is revealed if these are connected to the nearest indium atoms, as shown in Fig. 6 with the unique atoms labeled. This  $\text{In}_{48}\text{Na}_{12} = M_{60}$  cage is of the same shape as the  $C_{60}$  fullerene but the symmetry is reduced from the ideal  $I_h$  to  $C_{2v}$ . The cage is centered by the NiB-centered indium cluster (below) and fills the cavity discussed in the previous paragraph (Fig. 5). Each cage is connected to six other  $M_{60}$  cages through shared Na12–Na12 and Na48–Na48 edges (open tie lines, not bonds), their off-center locations allowing the connections to follow the wavy bilayers. The  $M_{60}$  is also fused to a pair of  $\text{In}_{78}$  fullerenes in the upper layer in Fig. 5 through shared pentagons In6, 22, 28, and to a pair of (inverted)  $\text{In}_{78}$  fullerenes in the lower layer through shared pentagons In2, 3, 23 (Fig. 3). The  $M_{60}$  cage is further fused to two  $\text{In}_{70}$  in the upper in Fig. 5 through shared pentagons In10, 21, 30 (Fig. 2). Finally, five of the 14 independent In atoms in the cage come from the  $\text{In}_3$  and  $\text{In}_6$  surface features. Notice in Fig. 6 that the sodium atoms lie a bit outside of the surface of the sphere defined by the indium atoms, and the pentagons, In18, 51, Na48 as an example, are puckered outward. The distortions result from Na–Na and Na–In distances being naturally longer than In–In. (A centered and condensed  $\text{In}_{48}\text{Na}_{12}$  cage between planar layers of condensed  $\text{In}_{74}$  cages is also found in  $\text{Na}_{96}\text{In}_{97}\text{Z}_2$  with the same types of face and edge sharing with other cages, but it has higher symmetry,  $D_{3d}$ .)

### Overall Packing

Since the bonding within the double layer of  $\text{In}_{70}$  and  $\text{In}_{78}$  has already been discussed in detail (Fig. 4), we will omit the exo In atoms that interconnect these layers from the following discussion and figures. Condensed views of the structure along or nearly along the axes  $a$ ,  $b$ , and  $c$  are shown in Figs. 7a, 7b, and 7c, respectively, with the different sized fullerenes labeled and the unit cell outlined. In order to show the positioning of the different cages rather than the fact that they are fused with each other, the sizes of the spheres that represent them have been reduced somewhat. We should remember that each type of cage is fused along  $a$  (Fig. 7b) with two like members, via pentagons for  $\text{In}_{78}$  and  $\text{In}_{70}$  and through pairs of sodium atoms for  $M_{60}$ . Also fused through pentagons are four  $M_{60}$  and four  $\text{In}_{70}$  cages about each  $\text{In}_{78}$  cage (10 total), two  $M_{60}$  and four  $\text{In}_{78}$  to each  $\text{In}_{70}$  (8 total), and two  $\text{In}_{70}$  and four  $\text{In}_{78}$  to each  $M_{60}$  plus six more  $M_{60}$  that only share edges. From Fig. 7c one can see that the individual layers of  $\text{In}_{70}$  and  $\text{In}_{78}$  (normal to  $c$ ) are, roughly speaking, close-packed in projection, that is, there are six spheres around each, two of the same and four of the other type. The spheres of



**FIG. 7.** (a) A condensed  $\sim[100]$  view of the unit cell, showing only the fullerenes as spheres. Rows of fullerenes of each type run parallel to the  $a$  axis, while rows of  $\text{In}_{70}$  and  $\text{In}_{78}$  alternate along the  $b$  axis (horizontal) and form close-packed but puckered layers that stack directly over each other. Layers of  $M_{60}$  fill the space between every other pair of  $\text{In}_{70}$  and  $\text{In}_{78}$  layers and assume the same wave-like pattern. The order of the stacking is  $\text{ABA}'\ddagger$ , where A and A' (reversed) are the  $\text{In}_{70}$ ,  $\text{In}_{78}$  layers, B is the  $M_{60}$  position, and  $\ddagger$  marks the omitted indium exo decorations around  $z = \frac{1}{2}$  (Fig. 1). (b) A condensed  $\sim[010]$  view of the unit cell. The rows of equivalent fullerenes parallel to the  $a$  axis (horizontal) can be seen as well as the stacking of the layers of fused  $\text{In}_{70}$  and  $\text{In}_{78}$  on top of each other. (c) A condensed  $[001]$  projection of the unit cell. Notice that the individual layers of fused  $\text{In}_{70}$  and  $\text{In}_{78}$  as well as the ones of  $M_{60}$  between them appear close-packed, although the layers are puckered.

each type form straight rows along the  $a$  axis (Fig. 7a), and these alternate and are waved along the  $b$  axis forming a wave-like surface (Fig. 7b). However, the neighboring layers of the same type are positioned exactly on the top of each other along  $c$  with  $\text{In}_{78}$  over  $\text{In}_{70}$ , etc. (Figs. 7a,b). Nominally close-packed layers of  $M_{60}$  are placed between every other pair of indium layers and take the wave-like shape defined by the latter.

We should point out here that  $\text{In}_{70}$  and  $C_{70}$  alike, with pseudo  $D_{5h}$  symmetry, have oblong rather than spherical shapes,  $\sim 16 \times 15 \text{ \AA}$  for the former. The long axis of the  $\text{In}_{70}$  ellipsoid happens to be equal to the diameter of the nearly spherical  $\text{In}_{78}$  of pseudo  $D_{3h}$  symmetry, and both are equal to the  $a$  axis of the unit cell. This coincidence and the fact that both cages have two diametrically opposed equatorial pentagons (along  $a$ , normal to  $c$ ) that can be shared with other cages of the same type are the grounds for the formation of commensurate rows of  $\text{In}_{70}$  and  $\text{In}_{78}$  along the  $a$  axis. The reason why the rows are ordered in a wave-like rather than planar fashion along the  $b$  direction originates in the absence of four more equatorial pentagons on these cages. Unlike the  $\text{In}_{74}$  ( $D_{3h}$ ) cage in  $\text{Na}_{96}\text{In}_{97}\text{Ni}_2$ , which has six pentagons in an equatorial plane and forms perfectly flat layers by sharing them with other  $\text{In}_{74}$  cages, the  $\text{In}_{70}$  and  $\text{In}_{78}$  have four additional pentagons outside

the waist (Figs. 2, 3). The layer formed by sharing them with other cages will automatically be puckered.

Were the mixed layers of  $\text{In}_{78}$  and  $\text{In}_{70}$  flat, they would form trigonal prismatic sites between them for  $M_{60}$ , since they stack exactly on top of each other in pairs (Fig. 7). The actual waving of the layers is such that one vertical edge of each trigonal prism is shifted up or down parallel to the  $c$  axis. A logical result of this is that the centering units are pushed toward the opposed rectangular face of the trigonal prism, and in the extreme case these species would center that face. The latter is the positioning of the  $M_{60}$  cages at the center of the rectangular faces formed between two  $\text{In}_{78}$ – $\text{In}_{70}$  vertical edges in a pseudo trigonal prism. The third (displaced) vertical edge is another pair of  $\text{In}_{70}$  and  $\text{In}_{78}$ . The packing scheme of the layers along the  $c$  axis is  $\text{ABA}'\ddagger\text{ABA}'\ddagger$ , where A is a  $\text{In}_{70}$ ,  $\text{In}_{78}$  layer, A' is that reversed, B is a  $M_{60}$  layer and  $\ddagger$  designates the position of the interconnecting In atoms around  $z = \frac{1}{2}$  (Figs. 1 and 4 but missing in Fig. 7).

#### Endohedral Sodium

The positioning of the sodium atoms throughout the structure is quite regular and significant in the ways these divide up space, similar to the disposition of cations in

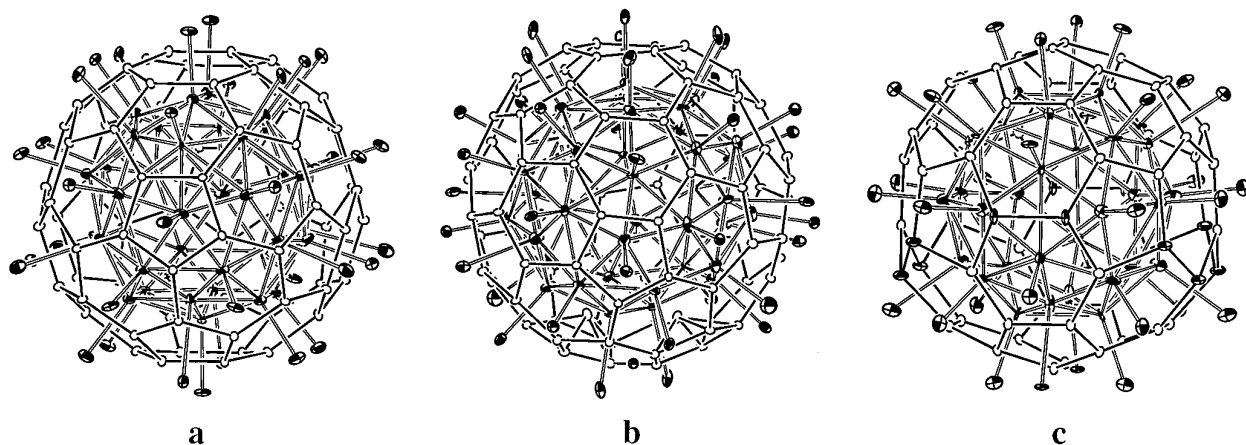


**FIG. 8.** (a) A view of the  $\text{In}_{70}$  fullerene (open ellipsoids, solid bonds) together with the nearest endo and exo sodium atoms (shaded circles) interconnected with double lines. All 37 pentagonal and hexagonal faces of the fullerene are thus capped from inside and outside by sodium in a duality role. The sodium atoms inside form a 37-atom deltahedron (also interconnected with double lines), while each of the 70 triangular faces of that deltahedron are capped by In. (b) A similar view of the  $\text{In}_{78}$  fullerene together with all nearest sodium atoms (shaded circles) interconnected by open "bonds." All 41 faces of the fullerene are capped from the inside by 39 sodium and 2 indium ( $\text{In}_{19}$ ) atoms which form a 41-atom *closo* deltahedron if all are included, or a 39-atom *arachno* deltahedron if the  $\text{In}_{19}$  atoms are excluded. All  $\text{In}_{78}$  faces capped by endo sodium are capped exo sodium atoms as well. (c) The  $M_{60}$  ( $= \text{In}_{48}\text{Na}_{12}$ ) fullerene (with In as open and Na as shaded ellipsoids) together with all nearest sodium atoms interconnected (open lines). All 32 pentagonal and hexagonal faces of the fullerene are endo- and exo-capped by sodium atoms. The sodium atoms inside form the 32 atom deltahedron marked with open interconnections. All 60 triangular faces of that deltahedron are capped by exo atoms of the  $M_{60}$ .

$\text{Na}_{96}\text{In}_{97}\text{Z}_2$ . Most of them are deployed to cap all hexagonal and pentagonal faces of the In cages from both sides, as shown in Fig. 8 for (a)  $\text{In}_{70}$ , (b)  $\text{In}_{78}$ , and (c)  $M_{60}$ . (Compare Figs. 2, 3, and 6, respectively.) A list of the capping atoms for all faces on these cages is available from the authors. There are 37 sodium atoms inside the 37 faces of  $\text{In}_{70}$ , 39 sodium atoms and 2 indium atoms ( $\text{In}_{19}$ ) inside the 41 faces of  $\text{In}_{78}$ , and 32 sodium atoms inside the 32 faces of  $M_{60}$ . The few remaining sodium atoms that do not cap faces of the fullerenes (Na10, 11, 23, 32, 37, 39, 47, 49, 57) are located near  $z = \frac{1}{2}$ , where they cap the faces of the linking deltahedra positioned there. In addition, Na18 caps all the exo hexagons In8, 8, 18, 18, 35, 35 (Fig. 5) that bridge between two  $\text{In}_{70}$  and one  $\text{In}_{78}$  cages in the In layers around  $z = 0$ .

If open lines are drawn between the sodium atoms inside of (endo to) the three different fullerene spheres, as in Fig. 8, additional nearly spherical formations inside all three are revealed. These are correspondingly regular 37-, 39-, and 32-atom deltahedra in which all sodium have five or six like neighbors, the inverse of the sizes of the faces they cap. The deltahedron inside the  $\text{In}_{78}$  cage, Fig. 8b, is *arachno*-type if only sodium atoms are considered, but it becomes *closo*-type when the two  $\text{In}_{19}$  atoms inside the  $\text{In}_{78}$  cage (labeled in Fig. 3) are included. Conversely, the In atoms in the fullerene cages can now be viewed as capping all triangles of the respective inner sodium deltahedra.

One very important consideration for later discussion is

that the endo-Na that cap larger hexagonal faces and thence have six-like neighbors lie closer to the surface of the fullerene, or farther from its center, than those endo-Na atoms that cap pentagonal faces, this being necessary in order to achieve more-or-less equal Na-In distances. (This also leads to shorter exo-endo Na-Na distances across the hexagons than across the pentagons.) This endohedral construction means that the positions of all inner sodium atoms within the fullerenes are fixed (determined) by the positions of the atoms building the cages. This feature will be seen to have dramatic effect on the isolated indium clusters that center all of these cages.

#### Centered Clusters

Finally, there are clusters within the endohedral sodium liners to the  $\text{In}_{70}$ ,  $M_{60}$ , and  $\text{In}_{78}$  fullerenes that are isolated in the sense that they are not bonded to any other indium units, namely, two different Ni-centered (NiA, NiB) and one Na1-centered (C) units, respectively. The well-defined Ni or Na core position in each is surrounded by a shell of electron density that for the most part lacks well-defined maxima, evidently because the indium cluster shell is partially disordered. These are quite spherical, with average radii of 2.73 (3), 2.86 (3), and 3.38 (5) Å around NiA, NiB, and Na1, respectively. The first two are quite appropriate for Ni-In distances when compared with the 2.77 Å average for  $\text{In}_{10}\text{Ni}^{10-}$  (6), and the third is common for Na-In separations (see Table 3). The electron densities within

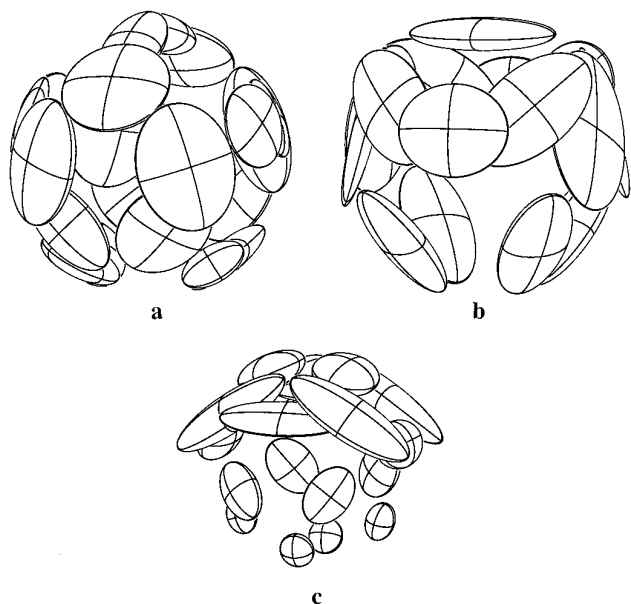


FIG. 9. Drawings at a 94% probability level of the refined indium atoms in the clusters centered by (a) NiA, (b) NiB, and (c) Na1 that are in turn encapsulated in the three fullerenes. Only a few islands on the surface of the first two and on the upper surface of the third one have nearly zero electron density.

these shells were approximated by placing indium atoms at all maxima and ultimately refining them anisotropically and with fractional occupancies. Figure 9 shows the results for the respective clusters when the ellipsoids are drawn at the 94% probability level. All ellipsoids around NiA and NiB and some around Na1 appear as two dimensional disks that are necessarily tangential to a sphere around the cluster center. The same three clusters are shown with 50% probability thermal ellipsoids in Fig. 10 where one can better see the more probable locations of the labeled indium atoms. The use of thermal ellipsoids to describe a partial spherical atom distribution of course carries some errors with it because of the use of planar (pancake-shaped) and centric electron density distributions and also in the underestimated shell radius it produces at the centroid.

*1. NiA-centered cluster.* The electron density around NiA (within  $In_{70}$ ) was refined with six independent indium positions, A1 to A6 (Fig. 10a). All of these sites refined with 50% occupancy (within  $1\sigma$ ) and yielded a sum of 10.0 (2) indium atoms per cluster (see Table 2). Some of the distances between them are, not surprisingly, quite small but many are suitable for In–In bonding separations in clusters. All of them are at reasonable distances from the central NiA (2.68 (1) to 2.801 (8) Å). The fact that each of the atoms of the cluster refined with half occupancy suggested that a good model might be a two-fold disorder of an  $In_{10}$  unit throughout the structure. The best model,

Figure 11a, is achieved by simple removal of duplicate atoms generated by the two vertical mirror planes through the Ni atom that are imposed by the space group. The view direction in Fig. 11a is slightly off that in Fig. 10a, but one can still see that this 10-atom cluster has half of each type of refined atom. All In–In distances (from 2.95 (1) to 3.35 (1) Å) but one are within the normal range, the exception being the InA2–InA3 distance which is 2.30 (41) Å, impossibly short for two indium atoms. Nevertheless, since all of the atoms of the cluster refine with such extreme thermal motions, it is possible that the microscopic positions of InA2 and InA3 in each  $In_{10}$  cluster are correlated and not actually at the centers of the refined ellipsoids. Each of these would only need to be moved about 0.3 Å in order to establish a reasonable bond length, while the radii of the disks approximating the distribution of InA2 and A3 (the largest in the cluster) are  $\sim 0.7$  Å even at the 50% probability level. The positions of all InA1–A6 atoms have been approximated in terms of the average positions for the same cluster disordered throughout the crystal, but it is possible to refine an atom artificially be-

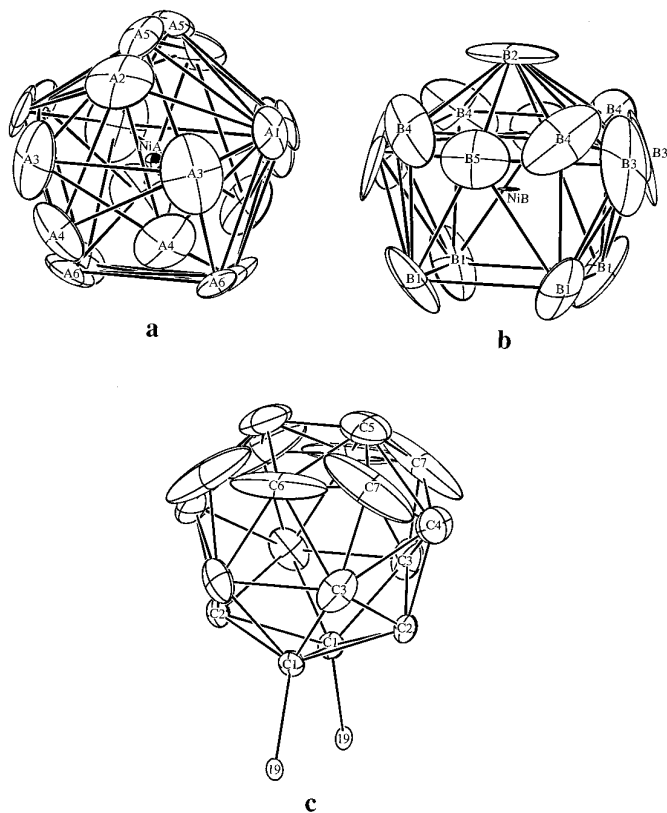


FIG. 10. The 50% probability thermal ellipsoid results for the encapsulated In clusters centered by (a) NiA, (b) NiB, and (c) Na1 (not shown) with neighbors interconnected. Note that the Na1-centered cluster (c) is two-bonded to a pair of In19 atoms which, in turn, are bound on the inner surface of the  $In_{78}$  fullerene (Fig. 3).

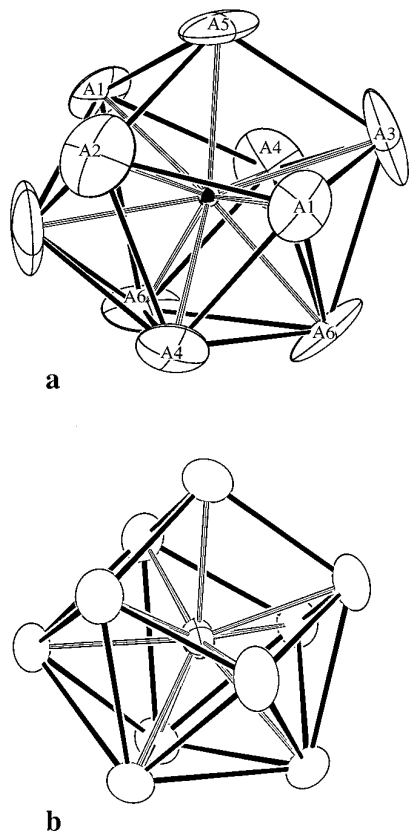


FIG. 11. (a) The geometry of a reasonable 10-atom model for the NiA-centered indium cluster in  $\text{In}_{78}$  (50% thermal ellipsoids) (see text) compared with that of (b) the  $\text{In}_{10}\text{Ni}^{10-}$  cluster A known in  $\text{K}_{10}\text{In}_{10}\text{Ni}$  (6) (94% thermal ellipsoids). Both are approximately tetrapped trigonal prisms ( $\sim C_{3v}$ , axis vertical).

tween two maxima in the electron density that are very close ( $0.3 \text{ \AA}$ ) to each other.

Assuming that the model we propose is correct, we can discuss the geometry of this cluster in terms of other examples. The Ni-centered isolated  $\text{In}_{10}\text{Ni}^{10-}$  cluster shown in Fig. 11b is, fortunately, already known in  $\text{K}_{10}\text{In}_{10}\text{Ni}$  (6). The two geometries are very close, and both can be considered as tetrapped trigonal prisms,  $\sim C_{3v}$ , with the axes vertical in the figure. The trigonal prism in Fig. 11a has atoms A4, A6, A6 as the base, A5 capping the large upper triangle A1, A2, A3, and atoms A1, A3, A4 capping all trapezoidal (formerly rectangular) faces of the trigonal prism. Since all atoms need to be nearly equidistant from the central nickel atom, the addition of capping atom A5 to the traditional tricapped trigonal prism causes expansion of the upper triangle (basal face). Extended-Hückel MO calculations for the cluster of Fig. 11b have shown that clusters with this geometry require  $2n = 20$  electrons for skeletal bonding, the Ni  $3d$  levels being low lying and closed shell. This yields an expected charge of  $-10$  for the  $\text{InNi}_{10}$  clusters encapsulated in  $\text{In}_{70}$ .

**2. NiB-centered cluster.** The electron density shell around NiB (within  $M_{60}$ ) was refined with five independent indium positions, Fig. 10b, B1 and B2 with 100% occupancy (within  $1\sigma$ ), and B3, B4 and B5 with 57(1), 35(1) and 70(1)% occupancies, respectively (Table 2). These yield a total of  $10.08(7)$  indium atoms per cluster. Again, some of the distances between the refined atom centroids are quite short but others are reasonable for In–In distances, and all of the indium atoms are at plausible distances from the central NiB atom ( $2.64(1)$  to  $2.699(8) \text{ \AA}$ ). As with the NiA-centered cluster, this one also can be modeled as a 10-atom indium cluster that is disordered throughout the structure but in a different orientation from that of Fig. 10b. The positional model shown in Fig. 12 is achieved by using all of the B1 and B2 atoms (100% occupancy) and one-half of each of the B3, B4 and B5 atom. The cluster in this orientation clearly resembles both the NiA-centered and the  $\text{In}_{10}\text{Ni}^{10-}$  clusters, Fig. 11, with B2, B3, B5 defining the base and one of the B1 atoms as the quasi-axial atom. The same charge is expected. The In–In distances range from  $2.94(1)$  to  $3.37(1) \text{ \AA}$  except for some relatively short separations, two of  $2.68(1) \text{ \AA}$  between InB1 and B3, two at  $2.76(1) \text{ \AA}$  between InB2 and B4, and a pair of  $2.78(2) \text{ \AA}$  length between InB3 and B4. Since most of the atoms of the cluster refined with very large tangential disks ( $10.7\text{--}18.0 \text{ \AA}^2$  for B2–B4), it is possible that the model atoms B1, B2, B3, and B4 in an actual cluster are slightly off the centers of the refined positions, as supposed with the NiA-centered cluster. Displacements of only  $\sim 0.1 \text{ \AA}$  for each of these atoms would make all distances “normal.” Note that the disordered model for cluster B was refined in  $C_{2v}$  symmetry with the principal axis through B2, a basal atom, while common rotation axes were present for the NiA-centered model.

This model for the NiB-centered cluster requires that

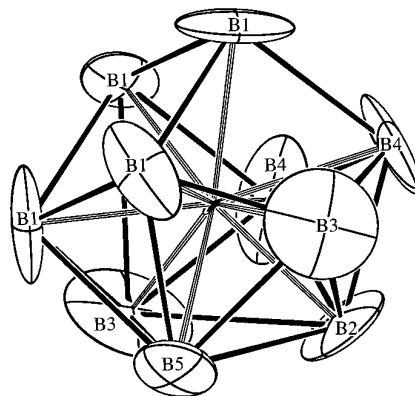
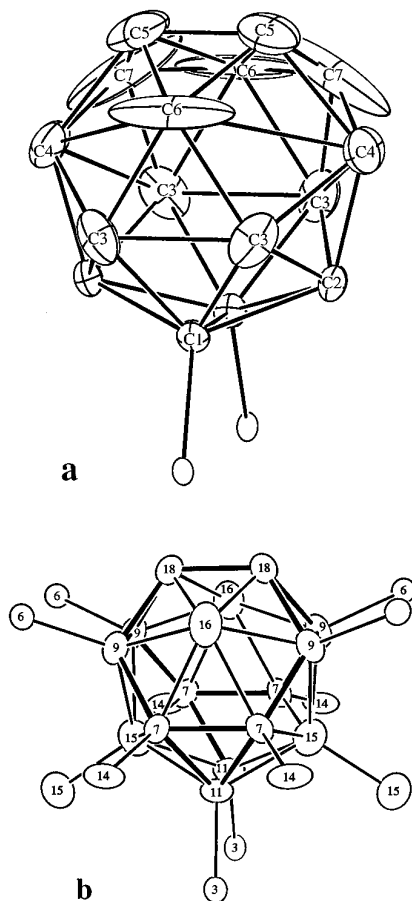


FIG. 12. A 10-atom model for the NiB-centered cluster with reasonable In–In distances. Its geometry is similar to that of the model for the NiA-centered cluster and the  $\text{In}_{10}\text{Ni}^{10-}$  cluster in  $\text{K}_{10}\text{In}_{10}\text{Ni}$  (Fig. 11). All are tetrapped trigonal prisms.

InB1 and B2 refine as 100% occupied, as they did, but that In B3, B4, and B5 should have been 50% occupied. These three in fact refined with 57(1), 35(1), and 70(1)% occupancies, respectively (a 54% average), which deviate correspondingly by  $7\sigma$ ,  $15\sigma$ , and  $20\sigma$  from the ideal values. The last two differences are quite large but, again, we should keep in mind that all of the so-called atoms of the refined cluster are imperfectly located, and they will, of course, affect the refined parameters of each other.

**3. NaI-centered cluster.** Cluster C, Fig. 10c, is nested near the center of the In<sub>78</sub> fullerane, but in an unusual way since it is directly bonded to the two endo In19 atoms on the latter (Fig. 3). The maxima in the electron density distribution around the central NaI atom for In atoms that lie nearer the attachments are quite well defined and have reasonable peak heights. On the other hand, more distant sections of the electron density have no clear maxima, but rather an almost continuous distribution with relatively low but not negligible heights, as if the cluster were “swinging” from its In19 tethers. Thus the atoms C1 to C3 refined with relatively normal thermal parameters and nearly full occupancies for indium, 100 (1)%, 100 (1)%, and 88 (1)%, respectively, the two InC1 atoms being the connections to In<sub>78</sub> via In19. C4 and C5 refined with smaller occupancies, 86 (2) and 78 (2)%, respectively ( $7\sigma$  and  $11\sigma$  from full occupancy), and their thermal parameters were quite large but not extreme ( $B_{\text{eq}} = 15, 18 \text{ \AA}^2$ ). Finally, C6 and C7 had very large and considerably elongated displacements with refined occupancies of 80 (1) and 50 (1)%, respectively. Two different cross-sections of the electron density distribution near InC6 and C7 (available from the authors) defined by the planes of InC4, C6, and C7, and for InC4, C5, and C7 (see Fig. 10c) show no well defined maxima near the positions refined for InC6 and, especially, C7, rather a more-or-less continuum in the shape of an arc that extends over InC4, C7, C6, C7, C4. Obviously, this behavior causes great problems when one tries to approximate it with a few discrete positions, and the result has large displacement ellipsoids and large ambiguities in the real positions of the atoms. Also, any artificial symmetry elements that pass through the center of the cluster will generate further problems since the refined positions will be some average and not necessarily correct.

We tried to model this cluster in a way similar to the Ni-centered examples above. A relatively reasonable result is shown in Fig. 13a, in which sites C1 to C6 are assumed to be fully occupied and C7 is half occupied (disordered). Removal of the imposed mirror plane near the printed page of Fig. 10c that disorders only C7 gives the model shown, a 2-bonded *closo*-In<sub>16</sub>. Of course, 78–88% occupancies refined for C3–C6 may mean that different *nido*, *arachno*, etc. species are actually present as well. Notwithstanding, Fig. 13b shows the very similar Na-centered, 12-bonded *closo*-In<sub>16</sub> ( $C_{2v}$ , icosioctahedron) that is already



**FIG. 13.** (a) The geometry of a 16-atom model for the two-bonded, NaI-centered indium cluster with reasonable In–In distances (compare Fig. 10c). The two unlabeled atoms are the In19 attachments to the In<sub>78</sub> cage. (b) The similar Na-centered, 12-bonded *closo*-In<sub>16</sub> ( $C_{2v}$ ) found in Na<sub>15</sub>In<sub>27.4</sub> (12). (Centering Na is not shown in either.)

known in Na<sub>15</sub>In<sub>27.4</sub> (12). (The exo bonding in the latter at In6, 14, and 15 is of no consequence here.)

Most of the distances in the modeled cluster for C as well as the two exo bonds are within the range of “normal” In–In distances, 2.80 (2) to 3.320 (9) Å. The two InC6–In4 distances drawn in front in the figure are very long, 4.49 Å. There are only six relatively short distances in the whole formation, two with 2.36 (2) Å for InC6–C7, two at 2.47 (2) Å for InC5–C7, and two of 2.58 (2) Å in InC4–C7. Notice that all of the latter include InC7, the atom with half occupancy and the most anisotropic “pancake” ( $B_{\text{eq}} = 27(1) \text{ \AA}^2$ ; rms  $\sim 0.6 \text{ \AA}$ ), so the distance problems do not seem very serious. The arguments that we used to rationalize short distances associated with atoms with large thermal ellipsoids in the other two clusters are valid here as well. A particular novelty of the In<sub>16</sub> cluster that has been deduced within the In<sub>78</sub> fullerane is that it hangs from the endo In19 attachments thereto, much like an oriole’s

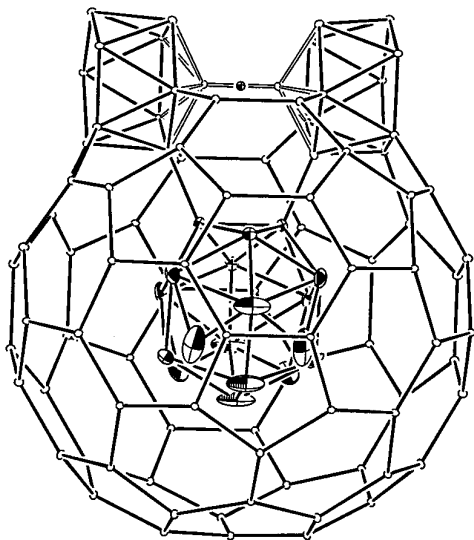


FIG. 14. The  $\text{In}_{16}$  cluster (shaded ellipsoids) that is suspended within the  $\text{In}_{78}$  cage via a pair of endohedral  $\text{In}_{19}$  atoms, “as an oriole’s nest.” The view is as refined, with duplicate  $\text{InC7}$  atoms (see text). The views of the two components are inverted from those shown in Figs. 3 and 13 (20% ellipsoids).

nest (Fig. 14). The relationship of this to examples of cages containing both unbonded and interconnected endohedral cluster arrays will be considered later.

#### Constraints on Cluster Order from Endohedral Sodium

Some good reasons for the limited disorder problems of the three nickel- or sodium-centered clusters can be found in the dimensional and symmetry constraints and conflicts that exist between the sodium sheaths inside the cages and the innermost clusters. A closer look at the electron density distributions on the entire Ni-centered clusters and on the upper part of the Na1-centered cluster (see Fig. 9) reveals that a few islands exist with nearly zero electron densities. Most of the surface is otherwise covered by the thermal ellipsoids of the atoms, especially when viewed at a 94% probability level. A second and particularly meaningful observation is that these islands of zero electron density are *always* located directly below the innermost sodium atoms in the exohedral sheath about each cluster. As noted earlier (5), those cations that cap pentagons on the In cage always lie somewhat further inside and appear in the sodium deltahedra with five neighbors, corresponding to the five hexagonal faces that share edges with the pentagon in the outer cage (Figs. 2, 3). Exactly the same positioning of “five-bonded” sodium atoms was observed earlier around isolated Z-centered indium clusters in  $\text{Na}_{96}\text{In}_{97}\text{Z}_2$  ( $Z = \text{Ni}, \text{Pd}, \text{or Pt}$ ), but the higher crystallographic symmetry at  $\text{In}_{74}$  ( $D_{3h}$ ) and  $M_{60}$  ( $D_{3d}$ ) therein made resolution of the refined disorder tentative and less convincing. Figures

15a,b,c shows the Na shells and the inner clusters **A**, **B**, **C** (in  $\text{In}_{70}$ ,  $M_{60}$  and  $\text{In}_{78}$ , respectively) at 94% probability levels. Here one can also perceive that the pentagon-capping sodium atoms in these lie much closer to the plane of the surrounding sodium pentagon and fall inside the best sphere defined by sodium with six neighbors. In a suitably “tight” cage, it should be impossible to locate an indium atom in an inner spherical cluster anywhere between the central Ni or Na atom and closer-lying sodium atoms that cap pentagons on the fullerane.

The veracity of this conclusion is made clear by the 50% probability drawings of the same inner three clusters in Fig. 16, where the radial connections between the central Ni or Na atom and only the pentagon-capping sodium atoms have been added. As seen, the inner In atoms more or less “float” on the surface of the cluster except that they are clearly excluded from the voids that lie radially below “five-bonded” sodium atoms. This explains some of the characteristics of the separate disk-like thermal ellipsoids that cover much of the surface of the refined clusters. Problems with the structure must arise from conflicts between the more or less  $C_{3v}$  symmetry of clusters **A** and **B** and the  $C_{2v}$  symmetry imposed by the In cage via the endohedral Na shell. Even so, the clusters inside the  $\text{In}_{70}$  and  $M_{60}$  cages (as well as within  $\text{In}_{74}$  and  $M_{60}$  in  $\text{Na}_{96}\text{In}_{97}\text{Z}_2$ ) have seemingly different refined geometries although all appear to be made of 10 indium atoms. While all of the cages have 12 pentagonal faces, these have different locations on the four cages so centered. In contrast, the sodium atoms on the inside of hexagons on the cages have reasonable distances to the indium beneath, sometimes on the short side (2.92 (2)–3.05 (1) Å in A, 2.86 (2)–3.04 (1) Å in B, 3.01(1) Å in C) but not particularly unreasonable relative to the shorter Na–In distances in  $\text{Na-In}_{11.8}$ , 3.06 and 3.12 Å (9). It should be remembered that the approximation of flat “pancakes” for the electron density arcs on the spheres will result in an underestimation of core–In distances near the center of the ellipsoid and the opposite error in the opposed  $d(\text{In-Na})$ . The former can also make the  $\text{NiIn}_{10}$  clusters therein seem compressed.

Notwithstanding, the average Ni–In distances do appear to vary with cage size. For  $M_{60}$  in  $\text{Na}_{96}\text{In}_{97}\text{Ni}_2$  (5) and  $\text{Na}_{172}\text{In}_{197}\text{Ni}_2$ , these are 2.59(2)–2.716(6) (2.66(3) Å average) and 2.64(1)–2.699(8) Å (2.67(3) Å, average), respectively, practically identical. The distances are apparently larger in bigger fullerenes;  $d(\text{Ni-In})$  is 2.68(1)–2.801(8) Å (2.73(3) Å average) in  $\text{In}_{70}$  and 2.67(1)–2.90(5) Å (2.78(3) Å average) in  $\text{In}_{74}$ . These suggest that the  $\text{In}_{10}$  clusters may be somewhat flexible in terms of Ni–In distances (as well as disorder) and that smaller fullerenes, which apply a higher degree of compression to the encapsulated and commensurate sodium deltahedra, in turn get closer to the indium atoms in the encapsulated clusters and effectively compress them and,

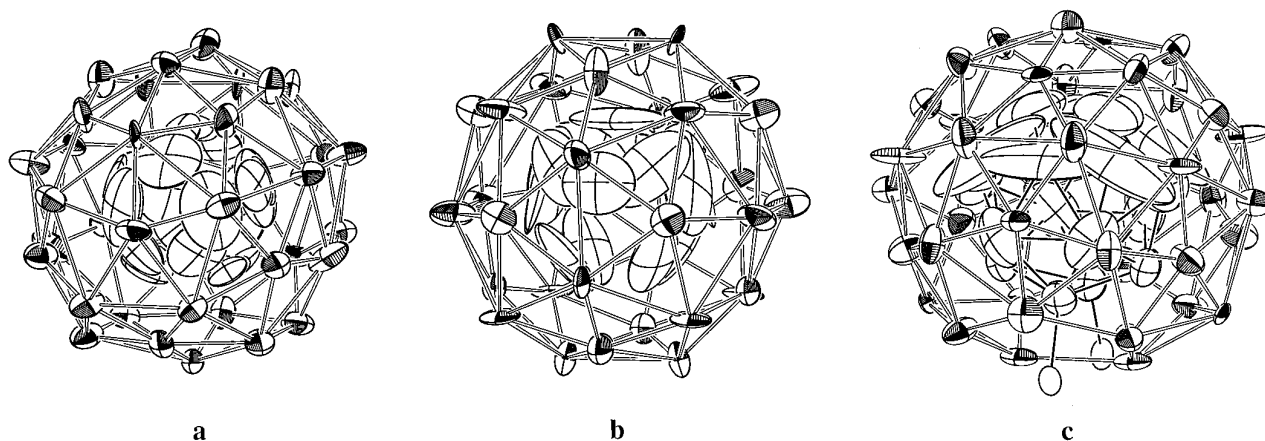


FIG. 15. The positioning of the sodium atom cage (shaded ellipsoids, open interconnections) around the isolated  $\text{NiIn}_{10}$  clusters (crossed ellipsoids) inside (a)  $\text{In}_{70}$  and, (b)  $M_{60}$ , and of  $\text{In}_{16}$  in (c)  $\text{In}_{78}$ , with the  $\text{In}_{19}$  tethers at the bottom. All of the sodium atoms that cap pentagons in the fullerenes lie above “openings” in the electron density on the surface of the clusters (94% thermal ellipsoids).

presumably, reduce the disorder somewhat. The applied symmetry of the gross structure may be more important in the last aspect, however.

The situation discussed above reminds one very much of so-called incommensurate structures. In the latter, the mismatch between layers or rows of atoms with different periodicities causes similar problems when refining the structure as commensurate. In our case, the mismatch is between the atoms of two spheres, the sodium cages which have fixed  $C_{2v}$  positions, and the  $\sim C_{3v}$  inner clusters, which are free to take different, but not all, orientations in respect to the first one. The incommensurability could be visualized as two incommensurate rows of atoms wrapped an infinite number of times around a sphere and could be called circular or angular incommensurability.

#### Fullerenes, Building Blocks, and Polyhedral Descriptions

Following the nomenclature proposed by Smalley and co-workers (21), the isolated, multiply endohedral  $\text{In}_{70}$  cage as an example can be written as  $Z@_{\text{In}_{10}}@_{\text{Na}_{37}}@_{\text{In}_{70}}$  where  $Z = \text{Ni}, \text{Pd}, \text{or Pt}$ . Of course, this oversimplifies a complex solid since these cages are not isolated but rather fused, not only with each other but with filled  $\text{In}_{78}$  and stuffed  $\text{In}_{48}\text{Na}_{12}$  cages as well, and all are decorated with smaller  $\text{In}$  units to give all indium at least four neighbors. Although they lack  $\pi$ -bonding, the cage shapes are clearly recognizable building blocks, and we continue to associate these structures with those proposed by the late Fuller by calling them “fullerenes.”

One other cage-built, endohedral compound is known besides  $\text{Na}_{96}\text{In}_{97}\text{Z}_2$  and  $\text{Na}_{172}\text{In}_{197}\text{Z}_2$ . Nesper in his *Habilitationschrift* (22) and later in a comment (7) described an unpublished structure that contains fused  $\text{Al}_{76}$  cages and has the approximate composition  $\text{LiMgAl}_2$ . Here  $\text{Al}_{76}$

cages of  $C_{3v}$  symmetry are fused through all twelve pentagonal faces to other cages of the same type to generate a c.c.p. solid. Unfortunately, only the  $\text{Al}$  sites that build the cages and a few unmixed  $\text{Li}$  and  $\text{Mg}$  sites have been unambiguously identified, but the doubly-endohedral building unit is clear and has been described as  $\text{Al}_3M_7@M_{46}@_{\text{Al}_{76}}$ , where  $M$  is mixed  $\text{Li}$  and  $\text{Mg}$ . The problems encountered in the refinement of the innermost cluster were similar to those reported here, and some apparent disorder that arises from some symmetry elements applicable only to the major structural components may again pertain. Nevertheless, this structure affords another example of the variety of large and novel cages found for heavier elements of the boron family. We can say “so long” to the uniqueness of the carbon fullerenes.

Nesper also noted some apparent similarities between the  $\text{In}$  and  $\text{Al}$  fullerane-type cages and other polyhedra in certain intermetallic compounds, some quasicrystalline-type compounds, and  $\beta$ -boron that raise questions about the uniqueness of the former group. We believe that more explicit discussion of this aspect is warranted. Many intermetallic compounds with relatively complicated structures have, for the purpose of easier comprehension, often been described in terms of different polyhedral blocks that are not the *real* repeating or building units. Rather, these are *imaginary* polyhedra, usually of high symmetry, that can be found on spheres (of appropriate radii) drawn around an atom or a high-symmetry position in the structure. A very important point that we would like to make here is that one and the same type of sphere can be drawn around many or all of the atoms or groups in these structures, which therefore means that these spheres overlap one another heavily and do not represent unique building blocks of the structure. For example, in the intermetallic com-



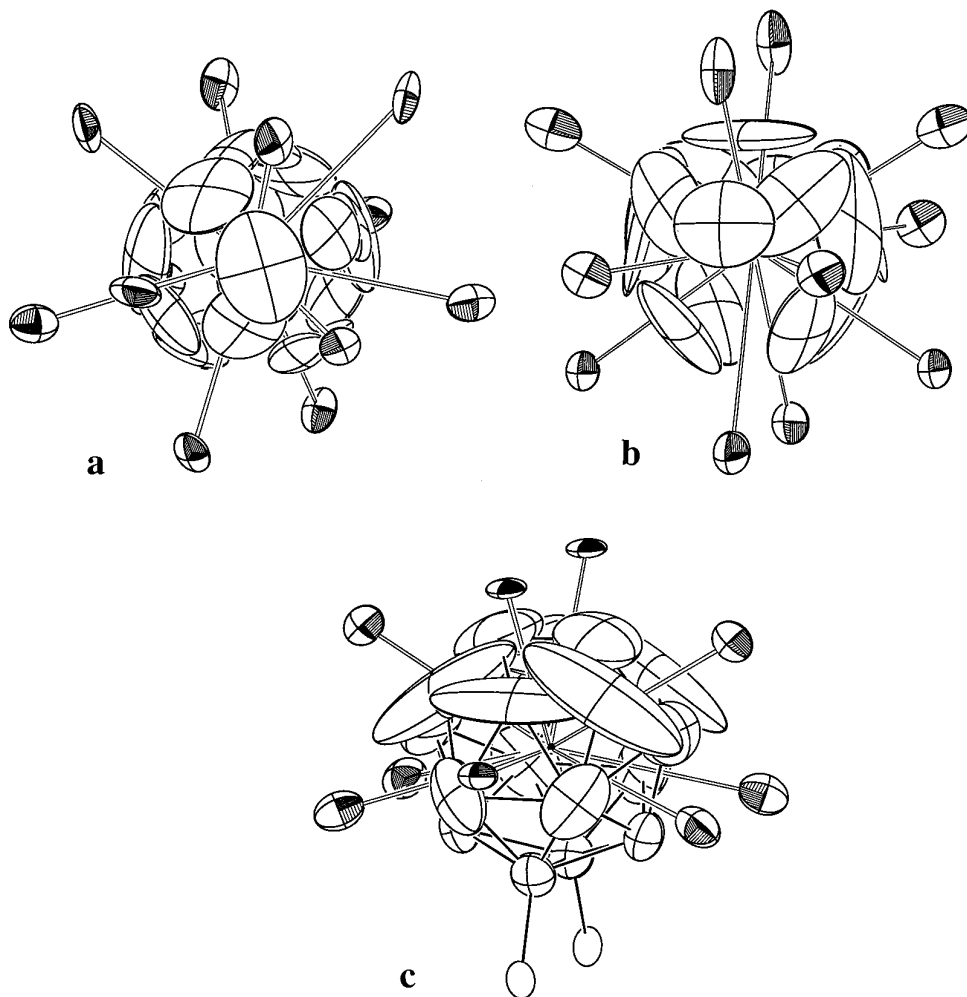


**FIG. 16.** The “five-bonded” sodium atoms (shaded ellipsoids) connected to the central atom by open lines, and the refined indium polyhedra thereabout, for (a) the NiAl, (b) NiB, (c) and NaI-centered clusters (74%). These Na–Z connections all pass through voids of nearly zero electron density on the refined indium cluster (crossed ellipsoids).

pound  $\text{Mg}_{32}(\text{Zn},\text{Al})_{49}$  (23), spheres can be drawn around the lattice points of a body-centered cube to define truncated icosahedra, that is, 60-atom fullerene-type formations (24). Nevertheless, the structure is not built of these formations, rather it is described as constructed of icosahedra or of “20 Friauf polyhedra that are arranged with their centers at the vertices of a pentagonal dodecahedron” (24). The structure actually contains icosahedra that are exo-bonded to 12 other icosahedra, and when the latter are cut by the appropriate sphere, the pentagonal faces of the 60-atom formation are produced—specifically, an 84-atom unit composed of a central icosahedron that is exo bonded to the apices of 12 pentagonal pyramids (inverted umbrellas) (24). The structure of  $\beta$ -boron ( $R = 105$ ) is of exactly the same character although half the outer units are more complex (8, 24). Many textbooks and articles describe imaginary 60 (or more) atom formations that can be found

in various structures when spheres with particular radii are drawn around the atoms. Again, this is done only to ease the comprehension of complicated structures;  $\beta$ -boron, as everyone knows, is built of interconnected icosahedra (and their trimers). On the other hand, the two indium structures presented here and described earlier (5) as well as the compound with a nominal composition “ $\text{LiMgAl}_2$ ” (21) are built of fullerane-type cages fused to each other, and there is no other way, easy or hard, to describe the structures. The true building units in these structures are the cages described, and any similarity to other descriptions of some intermetallic compounds and  $\beta$ -boron is only in the shape, not in the substance.

An even deeper look at the cage structures reveals some more interesting details that can be compared with the structure of, for example,  $\beta$ -boron. As mentioned above, if we draw a sphere with a particular radius around any

icosahedron in  $\beta$ -boron we will find a  $C_{60}$ -type cage with all pentagonal faces capped on the inside. In other words, the central icosahedron is 12-bonded to 12 more icosahedra that penetrate the  $B_{60}$  cage surface. The  $In_{70}$ ,  $In_{74}$ , and  $Al_{76}$  cages also have clusters at their centers ( $In_{10}Ni^{10-}$  and  $Al_3M_7$ ), but these are isolated and are not bonded to the surface. One can think of these as the extreme of the  $\beta$ -boron structure in which all cluster-to-surface bonds have been cut by “electronic scissors” (26), namely, the additional electrons made available by the cations. Such exo bonds from the inner cluster are needed when insufficient electrons are available, since each exo bond reduces each cluster charge (and therefore the need for extra electrons) by one. A particularly interesting situation which supports this way of thinking is presented within the fullerane  $In_{78}$  cage which is centered by a 16-atom cluster that is only two-bonded to two icosahedra fused to the surface of the cage (Fig. 14). This is very reminiscent of the  $\beta$ -boron connectivity but instead of 12 bonds to the surface, the central cluster now retains only 2, and instead of 12 icosahedra fused to the surface, the present cage has only 2. The result is therefore in between the two extremes, those without any connections ( $In_{70}$ ,  $In_{74}$ , and  $Al_{76}$ ) and the one in which all vertices of the central cluster connected to the surface ( $\beta$ -boron,  $Mg_{32}(Zn,Al)_{49}$ , etc.). Apparently there are not enough additional electrons to cut the last two bonds to the central cluster in  $In_{78}$ . This is supported by the stoichiometry of the present compound compared with that of  $Na_{96}In_{97}Ni_2$  and “ $LiMgAl_2$ .” The present phase has approximately 0.87 additional electrons per In atom, while this number is about unity or higher for the other two. Thus the “electronic scissors” have only been partially effective in isolating cluster units. A great many heavily interlinked polyhedral networks of gallium and indium occur when only lower electron counts per triel element are available (27,28).

## CONCLUSION

The general chemistry of indium in negative oxidation states shows a remarkable diversity. This spans from truly intermetallic compounds, such as  $KIn_4$  and  $RbIn_4$  ( $BaAl_4$ -type structures) (29), with metallic and more or less nondirectional type bonding of 8-coordinate indium atoms, to molecular ions in  $Na_2In$  (12) where covalent (directional) three-bonded In atoms form  $In_4^{-8}$ . Moreover, the range of oxidation states possible provides a large number of compounds with different structures and similar stoichiometries. The ability of indium to take on three-, four-, five-, six- and even seven-bonded motifs in one and the same compound produces an amazing structural variety. Simply by increasing or decreasing the ratio of less-bonded to more-bonded atoms, the compounds can in parallel accommodate

more or fewer electrons. In other words, an almost continuous range of compounds would in principle be possible between the structures of  $KIn_4$  and  $Na_2In$  if there was room for any particular number of cations. A very good example is the existence of the compounds  $K_{22}In_{39}$  and  $K_{15}Na_8In_{39}$  in which one additional electron in the second causes two four-bonded indium atoms to become three-bonded and two six-bonded indium atoms to become five-bonded while the rest of the network structure remains the same (11). Notice that the difference in the stoichiometries of the two compounds is only one cation out of 61 or 62 atoms.

Another structural advantage for indium, but not only for indium, is its ability to mimic some of the structural specificities of the elements of main-group tetrels (Tt, group 14). As an example,  $In^-$  (electronically equivalent to  $Tt^0$ ) forms a diamond-type network in  $NaIn$  ( $NaTi$ -type) (30) and  $In^{2-}$  (electronically equivalent to  $Tt^{1-}$ ) forms tetrahedra, as does  $Sn^-$  in  $NaSn$  (12, 31). It is not so surprising, then, that indium with an oxidation state in the neighborhood of  $-1$  can also form fullerane-type structures related to those of carbon, although the cages in the former are large and need to be propped open, and the absence of  $\pi$ -bonding requires other modifications. Different sized, fullerane-type indium cages form around nucleation centers such as Ni, Pd, Pt that are already known for their tendency for cluster centering in the presence of enough alkali-metal atoms (electrons) to provide a nearly  $-1$  formal charge on the indium atoms (mostly four-bonded). The sizes of these cages and the connectivity between them presumably depend upon many factors besides space-filling efficiency, and the complexities of the present structure testify to the many possibilities. Conversely, it is remarkable how many complexities are introduced in order to fulfil, or approach, valence rules as well as good space-filling, cation valence needs, and periodicity (9,28). Another variable is the formal oxidation state of indium, that is, the atomic Na:In ratio. The value for the indium atoms in  $Na_{96}In_{97}Ni_2$  is practically  $-1$ , and therefore mainly 4-bonded indium atoms are expected throughout the structure. Indeed, only 14 of the 77 indium atoms (18%) in the fused 74-atom fullerane network have more than four bonds (neighbors) (12 are 5- and 2 are 6-bonded). In  $Na_{172}In_{197}Z_2$ , the ratio Na : In is less, 0.87 : 1.0, and therefore more indium atoms have more bonds. Out of the 174 that build the fused 70- and 78-atom fullerenes, 46 are 5- and 26 are 6-bonded, 41% overall.

The triel metals Ga and Tl likewise exhibit distinctive anionic cluster chemistries as well (28). Gallium forms a very large variety of interbonded and fused cluster networks (27), but nothing so far resembling a fullerane architecture. In contrast, thallium exhibits a considerable range of discrete clusters from  $Tl_4^{8-}$  up, some centered but so far none larger than  $Tl_{13}^{11-}$ , and only a few network

examples (32–34). It is the unprecedentedness and the variety that keep us interested!

### ACKNOWLEDGMENT

We are indebted to Victor Young for providing a CAD4 diffractometer in excellent operating condition.

### REFERENCES

- G. S. Hammond, and V. J. Kuck, (Eds.), "Fullerenes: Synthesis, Properties and Chemistry of Large Carbon Clusters" American Chemical Society Symposium Series, Vol. 481. Am. Chem. Soc., Washington, DC, 1992.
- W. E. Billups and M. A. Ciufolini (Eds.), "Buckminsterfullerenes." VCH, Weinheim, 1993.
- H. W. Kroto, J. E. Fischer, and C. E. Cox, (Eds.), "The Fullerenes." Pergamon, Oxford, 1993.
- F. T. Edelmann, *Angew. Chem. Int. Ed. Engl.* **34**, 981 (1995).
- S. C. Sevo and J. D. Corbett, *Science*, **262**, 880 (1993).
- S. C. Sevo and J. D. Corbett, *J. Am. Chem. Soc.* **115**, 9089 (1993).
- R. Nesper, *Angew. Chem. Int. Ed. Engl.* **33**, 843 (1994).
- W. B. Pearson, "The Crystal Chemistry and Physics of Metals and Alloys," pp. 31 and 296. Wiley, New York, 1972.
- S. C. Sevo and J. D. Corbett, *Inorg. Chem.* **31**, 1895 (1992).
- G. M. Sheldrick, "SHELXS-86." Universität Göttingen, Germany, 1986.
- S. C. Sevo and J. D. Corbett, unpublished research.
- S. C. Sevo and J. D. Corbett, *J. Solid State Chem.* **103**, 114 (1993).
- Z.-C. Dong and J. D. Corbett, *Inorg. Chem.* **34**, 5709 (1995).
- P. W. Fowler, R. C. Batten, and D. E. Manolopoulos, *J. Chem. Soc. Faraday Trans.* **87**, 3103 (1991).
- X. Liu, T. G. Schmalz, and D. J. Klein, *Chem. Phys. Lett.* **188**, 550 (1992).
- B. L. Zhang, C. Z. Wang, and K. M. Ho, *Chem. Phys. Lett.* **193**, 225 (1992).
- F. Diederich, R. L. Whetten, C. Thilgen, R. Ettl, I. Chao, and M. M. Alvarez, *Science*, **254**, 1768 (1991).
- J. R. Colt and G. E. Scuseria, *Chem. Phys. Lett.* **199**, 505 (1992).
- K. Kikuchi, N. Nakahara, T. Wakabayashi, S. Suzuki, H. Shiromaru, Y. Mijake, K. Saito, I. Ikemoto, M. Kainosho, and Y. Achiba, *Nature* **357**, 142 (1992).
- Z.-C. Dong and J. D. Corbett, *Inorg. Chem.*, in press.
- T. Guo, C. Jin, and R. E. Smalley, *J. Phys. Chem.* **95**, 4948 (1991).
- R. Nesper, *Habilitationschrift*. Universität Stuttgart, Germany (1988).
- G. Bergman, J. L. P. Waugh, and L. Pauling. *Acta Crystallogr.* **10**, 254 (1957).
- S. Samson, *Mater. Sci. Forum* **22–24**, 83 (1987).
- J. Donahue, "The Structures of the Elements," pp. 61–78. Wiley, New York, 1974.
- J. K. Burdett, *Nature* **279**, 121 (1979); private communication.
- C. Belin and M. Tillard-Charbonnel, *Prog. Solid State Chem.* **22**, 59 (1993).
- J. D. Corbett, in "Chemistry, Structure and Bonding in Zintl Phases and Ions," (S. M. Kauzlarich, Ed., Chap. 4. VCH, Weinheim, in press.
- R. Thümmel and W. Klemm, *Z. Anorg. Allg. Chem.* **376**, 44 (1970).
- E. Zintl and S. Neumayr, *Z. Phys. Chem. Abt. B* **20**, 272 (1933).
- W. Müller and K. Volk, *Z. Naturforsch. B* **32**, 709 (1977).
- Z.-C. Dong and J. D. Corbett, *J. Am. Chem. Soc.* **116**, 3429 (1994).
- Z.-C. Dong and J. D. Corbett, *J. Am. Chem. Soc.* **117**, 6447 (1995).
- Z.-C. Dong and J. D. Corbett, *Inorg. Chem.*, **35**, 1444 (1996).